Aus der Fachrichtung Biophysik

Theoretische Medizin und Biowissenschaften der

Medizinischen Fakultät der Universität des Saarlandes,

Homburg/Saar

Effects of noise traumata of different strengths on hearing functions of C57BL/6N mice

Dissertation zur Erlangung des Grades eines Doktors der

Medizin der Medizinischen Fakultät der Universität des

Saarlandes 2025

vorgelegt von

Philip DERLEDER

Geboren am 19.06.1970 in Kiel

Dekan der Medizinischen Fakultät Prof. Dr. med. dent. Matthias Hannig

Die Dissertation „Effects of noise traumata of different strengths on hearing functions of C57BL/6N mice" wurde in der Arbeitsgruppe von Frau Prof. Dr. Jutta Engel am Centrum für Integrative Physiologie und Molekulare Medizin (CIPPM) in der Fachrichtung Biophysik angefertigt.

Table of contents

1 Figures, Tables and Abbreviations

1.1 Figures

1.2   Tables

Table 1: Statistical analysis of the effects of the 112 dB SPL trauma on f-ABR thresholds on days -2 and 28

Table 2: Statistical analysis of the initial f-ABR thresholds on day -2

Table 3: Statistical analysis the effect of trauma strength on f-ABR thresholds on day 28

Table 4: Statistical analysis of the effect of trauma strength on frequency-specific threshold shifts between day -2 and day 28

Table 5: Statistical analysis of the strength of noise trauma on frequency-specific threshold shifts between day -2 and day 1 after trauma

Table 6: Statistical analysis of the strength of noise trauma on frequency-specific threshold shifts between day -2 and day 14 after trauma

Table 7: Effects of trauma strength on recovery of f-ABR thresholds one day after trauma

Table 8: Effects of trauma strength on recovery of f-ABR thresholds 14 days after trauma

Table 9: Effects of trauma strength on recovery of f-ABR thresholds 28 days after trauma

Table 10: Detailed pair analysis of the Friedman/Bonferroni test of peak latencies of wave I in the 106 dB SPL trauma group

Table 11: Statistical analysis (Wilcoxon signed test) of the level-dependent wave I amplitudes before and 28 days after the 106 dB SPL trauma

Table 12: Statistical analysis (Wilcoxon signed test) of the level-dependent wave I amplitudes before and 28 days after the 112 dB SPL trauma

Table 13: Statistical analysis (Wilcoxon signed test) of the level-dependent wave I amplitudes at 11, 16, and 22 kHz before and 28 days after the 106 dB SPL trauma

Table 14: Reduction of mean amplitudes of Wave I on day 28 compared with day -2 for 11, 16, and 22 kHz

Table 15: Number of ears measured in the 106 dB SPL trauma group at 32 kHz

Table 16 (annex): Detailed pair analysis of the Friedman/Bonferroni test between day -2 versus any post-traumatic day of latencies in waves I-V in the two trauma groups

1.3 Abbreviations

ABR	Auditory brainstem response
AHL	Age related hearing loss
ANF	Auditory nerve fiber
BERA	Brainstem evoked response audiometry
BM	Basilar membrane
Cand. med.	Candidate of Medicine. Title of a medical student in Germany´s current six-year program who passed the First Medical State Exam
C57Bl/6N	C57 Black6N mouse strain
dB SPL	Decibel sound pressure level
DPOAE	Distortion product otoacoustic emissions
f-ABR	frequency-ABR
Fig.	Figure
HSR	High spontaneous rate
Hz	Hertz
IHC	Inner hair cells
kHz	kilohertz
LSR	Low spontaneous rate
mM	millimol per liter
MSR	Medium spontaneous rate
NIHL	Noise induced hearing loss
NIHHL	Noise induced hidden hearing loss
ns	not significant
OHC	Outer hair cells
OSHA	Occupational Safety and Health Administration
OW	Oval window
Pascal	Pa
PTS	Permanent threshold shift
RM	Reissner membrane
SD	Standard deviation
SG	Spiral ganglion
SGC	Spiral ganglion cell
SM	Scala media
SPL	Sound pressure level
SR	Spontaneous rate
Stud. med.	Student of medicine. Title of a medical student in Germany´s current six-year program who has not passed the First Medical State Exam

SV	Scala vestibuli
TM	Tectorial membrane
TTS	Temporary threshold shift
V	Volt

2 Summary

Noise-induced hearing loss is a common pathology in humans. Mice serve as model organism for unraveling the underlying mechanisms. Moderate noise (100 dB SPL, 2 h, 8 -16 kHz) can irreversibly damage the cochlea by destroying part of the presynapses and/or postsynapses of the inner hair cells in the high frequency region without permanently increasing hearing thresholds. This phenomenon termed hidden hearing loss was first demonstrated by Kujawa and Liberman (2009) in CBA/CaJ mice. The C57BL/6N mouse line has been widely used for genetic manipulation, e.g. for generating knock-out and knock-in mice, which can help to gain mechanistic insights into noise-induced hearing loss. The aim of this thesis was to explore hearing function after application of two different noise traumata - 106 and 112 dB SPL - in C57BL/6N mice.

Hearing function was assessed two days before, directly after trauma and up to four weeks after trauma by auditory brainstem response (ABR) audiometry with click and pure tone stimulation. A previously applied noise trauma of 100 dB SPL (2 h, 8-16 kHz octave band, (Nasri, 2023)) caused a permanent threshold shift at 45 kHz in C57BL/6N mice. The more intense traumata applied in this study (106 and 112 dB SPL) caused a larger damage. Both the amount of temporary (TTS) as well as permanent threshold shifts (PTS) and the range of affected frequencies scaled with trauma strength. In the case of TTS, recovery was almost complete on day 14. Four weeks after the 106 dB SPL trauma, the amplitude growth functions of ABR waves I were reduced for the frequencies of 11, 16, and 22 kHz, which indicates loss of functional synaptic connections between inner hair cells and spiral ganglion neurons. In a fellow dissertation, Philipp Schätzle showed trauma-induced loss of ~50 % of synaptic ribbons in inner hair cells in the mid-basal region (Blum et al., 2024), which was largely responsible for the reduction of the amplitude of ABR wave I by 72 % at 22 kHz four weeks after the 106 dB SPL trauma.

Similarly, growth functions of ABR wave I amplitudes evoked by click stimulation were reduced four weeks after both the 106 and the 112 dB SPL trauma. Mean amplitudes of click-ABR 40 dB over threshold were reduced for the waves I to V four weeks after the 106 dB SPL trauma and for waves I, III, IV, and V four weeks after the 112 dB SPL trauma. By contrast, peak latencies of waves I to V at 40 dB over threshold were not altered by either trauma suggesting that latencies of click responses relative to threshold are not a sensitive measure for loss of functional connections between inner hair cells and spiral ganglion neurons.

Although both the 106 and the 112 dB SPL trauma did not cause cellular outer hair cell loss (Blum et al., 2024) a functional impairment of outer hair cells is likely, which will lead to increased hearing thresholds independent of the loss of threshold-determining auditory nerve Ia

fibers. Future studies on hidden and overt hearing loss in genetic mouse models therefore should not only analyze ABR properties and the fate of pre- and postsynapses but also include measurements of the distortion product otoacoustic emissions as an indicator of outer hair cell function.

2.1 Zusammenfassung

Auswirkungen von Schalltraumata unterschiedlicher Stärke auf die Hörfunktion der Mauslinie C57BL/6N

Lärmbedingter Hörverlust ist ein häufig auftretendes Krankheitsbild beim Menschen. Beobachtungen an Mäusen ermöglichen die Aufdeckung der damit zugrunde liegenden Mechanismen. Ein mittelgradiges Lärmtrauma (100 dB SPL, 2 h, 8 -16 kHz) kann einen irreversiblen Schaden am Hörorgan verursachen, ohne dauerhaft die Hörschwellen zu erhöhen. Dieses als versteckter Hörverlust benannte Phänomen geschieht durch die Zerstörung von einem Teil der Präsynapsen und/oder der Postsynapsen der inneren Haarzellen in der Hochfrequenzregion. Es wurde erstmals in einer Veröffentlichung von Kujawa und Libermann aus dem Jahre 2009 an Mäusen der CBA/CaJ-Linie beschrieben. Die Mauslinie C57BL/6N ist ein häufig genutzter Stamm für genetische Manipulationen, z.B. für die Generierung von knock-out- und knock-in-Mausmodellen, die zur Aufklärung der Mechanismen von lärmbedingtem Hörverlust genutzt werden können. Das Ziel dieser Arbeit war die umfassende Analyse der Hörfunktion bei C57BL/6N-Mäusen nach zwei verschiedenen Lärmtraumata - 106 und 112 dB SPL.

Die Hörfunktion wurde zwei Tage vor, direkt dem Schalltrauma anschließend und bis vier Wochen danach durch Auditory Brainstem Response (ABR)-Messungen mit Klickgeräuschen (breites Frequenzspektrum) und monofrequenten Tönen untersucht. Ein vorausgegangenes Experiment mit einem Lärmtrauma von 100 dB SPL (2 h, 8-16 kHz Oktavband, (Nasri, 2023)) hatte bei C57BL/6N-Mäusen eine dauerhafte Erhöhung der Hörschwelle bei 45 kHz-Tönen verursacht. Die intensiveren Schalltraumata dieser Studie (106 und 112 dB SPL) erzeugten noch größere Schäden. Sowohl das Ausmaß der vorübergehenden (TTS) und dauerhaften Erhöhung der Hörschwellen (PTS) als auch die Anzahl der betroffenen Frequenzen nahm abhängig von der Traumaintensität zu. Im Falle einer nur vorübergehenden Erhöhung der Hörschwellen (TTS) erfolgte eine fast komplette Erholung der Hörfunktion nach 14 Tagen. Vier Wochen nach dem 106 dB SPL-Schalltrauma zeigten sich reduzierte Wachstumsfunktionen der ABR-Welle I bei bestimmten Frequenzen (11, 16 und 22 kHz). Dies weist auf einen Verlust von funktionierenden Synapsen zwischen inneren Haarzellen und Neuronen der Spiralganglien hin. Philipp Schätzle zeigte in seiner Dissertation, dass circa 50% der synaptischen Kontaktstellen (Ribbons) der inneren Haarzellen der mittleren basalen Region durch das Trauma verloren gingen (Blum et al., 2024). Dies erklärt größtenteils den Abfall der Amplitude der ABR-Welle I um 72 % bei 22 kHz vier Wochen nach dem 106 dB SPL-Schalltrauma.

Vier Wochen nach den Schalltraumata (106 und 112 dB SPL) waren die Wachstumsfunktionen der ABR-Welle I bei Klick-Stimulation ähnlich vermindert. In der 106 dB SPL-Traumagruppe waren die durchschnittlichen Amplituden nach Klickgeräuschen 40 dB über der Hörschwelle

bei allen ABR-Wellen (I-V) vermindert. Ähnliches zeigte sich in der 112 dB SPL-Traumagruppe, wo die ABR-Wellen I, III, IV und V vermindert waren (jeweils vier Wochen nach dem Trauma). Im Gegensatz dazu wurden die Peak-Latenzen der ABR-Wellen I-V bei Klick-geräuschen 40 dB über der Hörschwelle nicht durch die Traumata verändert. Daraus lässt sich schließen, dass diese Art der Latenzmessung kein sensitives Maß für den Verlust funktioneller Kontakte zwischen inneren Haarzellen und Spiralganglien ist.

Die 106 und 112 dB SPL Schalltraumata verursachten keinen Verlust der äußeren Haarzellen (Blum et al., 2024). Allerdings ist in der Folge eine Funktionsminderung mit erhöhten Hör-schwellen wahrscheinlich, unabhängig von einem Verlust der schwellenbestimmenden Ia-Fa-sern der Hörnerven. Zukünftige Studien über offenen und versteckten Hörverlust an geneti-schen Mausmodellen sollten nicht nur ABR-Charakteristika und das histologische Schicksal der Prä- und Postsynapsen analysieren. Das Augenmerk sollte sich ebenfalls auf Messungen von DPOAE (distortion product otoacoustic emissions) richten, welche die Funktionstüchtigkeit der äußeren Haarzellen widerspiegelt.

3 Introduction

3.1 Anatomy and physiology of the hearing organ

When molecules in the air surrounding us collide with their neighbors, they produce air pressure. It is measured in Pascal (1 Pascal = 1 Newton/m^2). Through the auditory sense in mammals, changes in air pressure are experienced as sound. Atmospheric pressure is approximately 100,000 Pascal (Pa) at sea level. Yet a change of 20 µPa, a fractional change of 2 parts in 10 billion, can be heard by young humans in their most favorable hearing range (Geisler, 1998). On the level of the basilar membrane of the inner ear, displacement amplitudes at threshold are of atomic dimensions (Fettiplace, 2017).

This wide range of pressures is best displayed through a logarithmic scale. The reference pressure of 20 µPa mentioned above is 0 dB SPL. For historical reasons the logarithmic number is multiplied by 20 and given the units of decibels sound pressure level (dB SPL). This means a pressure of 200 µPa has a value of 40 dB SPL. For humans the range of sound pressure extends from 0 dB SPL to 140 dB SPL, the latter is painfully loud.

When sound pressure waves arrive in the ear, the external (or outer) ear has the role to collect them and channel them forward (Figure 1). Having two ears enables mammals to compare two samples of incoming sounds. It can serve as source localization through a time difference in arrival of sound waves. As a collecting horn, it can increase the sound pressure on the ear drum.

The ear drum and middle ear ossicles transform the mechanical energy of sound, channeling it to the oval window of the cochlea. The middle ear anatomy cannot prevent a certain degree of sound reflection due to impedance jumps. But its unique structure with the ossicles amplifies and adapts, using lever action. There are two middle ear muscles (m. stapedius and m. tensor tympani) that are capable of partially blocking transmission of sound by stiffening the ossicles' chain (Brask, 1978; Gnadeberg et al., 1994; Snow et al., 2009). This is especially valid for low-frequency, high-intensity sounds. These muscles have a modified activity during anesthesia, as discussed in Chapter 6.
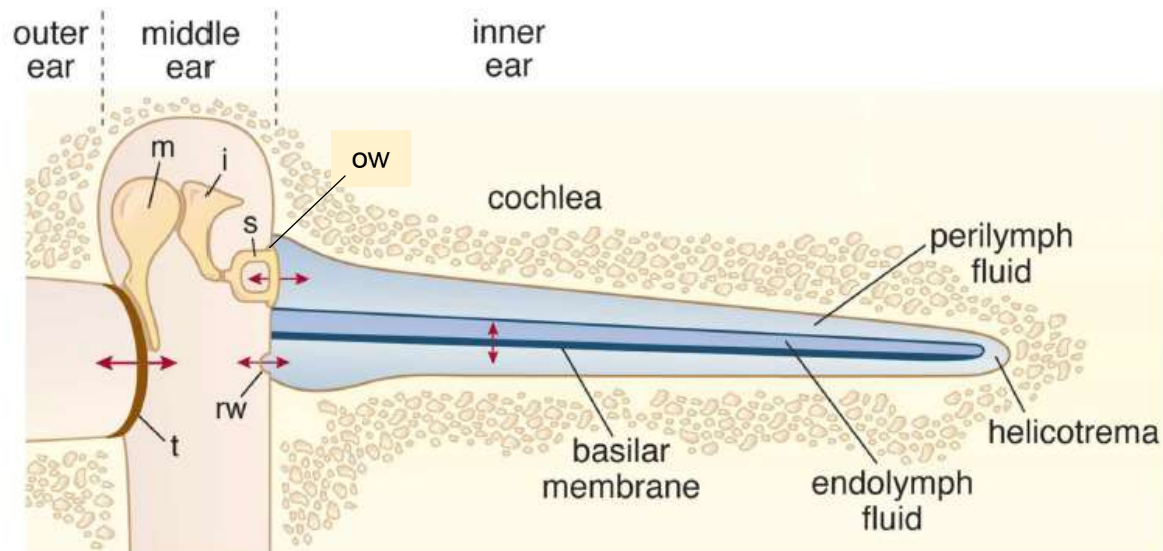
Figure 1. Simplified scheme of the ear. For clarity, the cochlea is straightened. Its three compartments contain either perilymph or endolymph fluid. In mice, the cochlea measures 6 mm, in humans 35 mm. Tympanum (t), malleus (m), incus (i), stapes (s), oval window (ow) and round window (rw). Figure from (Fettiplace, 2017).

The cochlea is the auditory part of the inner ear. Though cochlear sizes and frequency ranges of hearing differ between mammalian species, there is great uniformity in the structure of mammalian cochleae (Lorimer et al., 2015). This is coupled with an approximately 99% genetic match between humans and mice in this domain, termed as orthology (Scimemi et al., 2014). Analyzing the effects of for example noise exposure in mice can give us important clues for research and evaluation of the human inner ear. More specifically, animal experiments are indispensable in promoting development of pharmaceuticals, diagnosis and therapies for humans (Kujawa and Liberman, 2019).
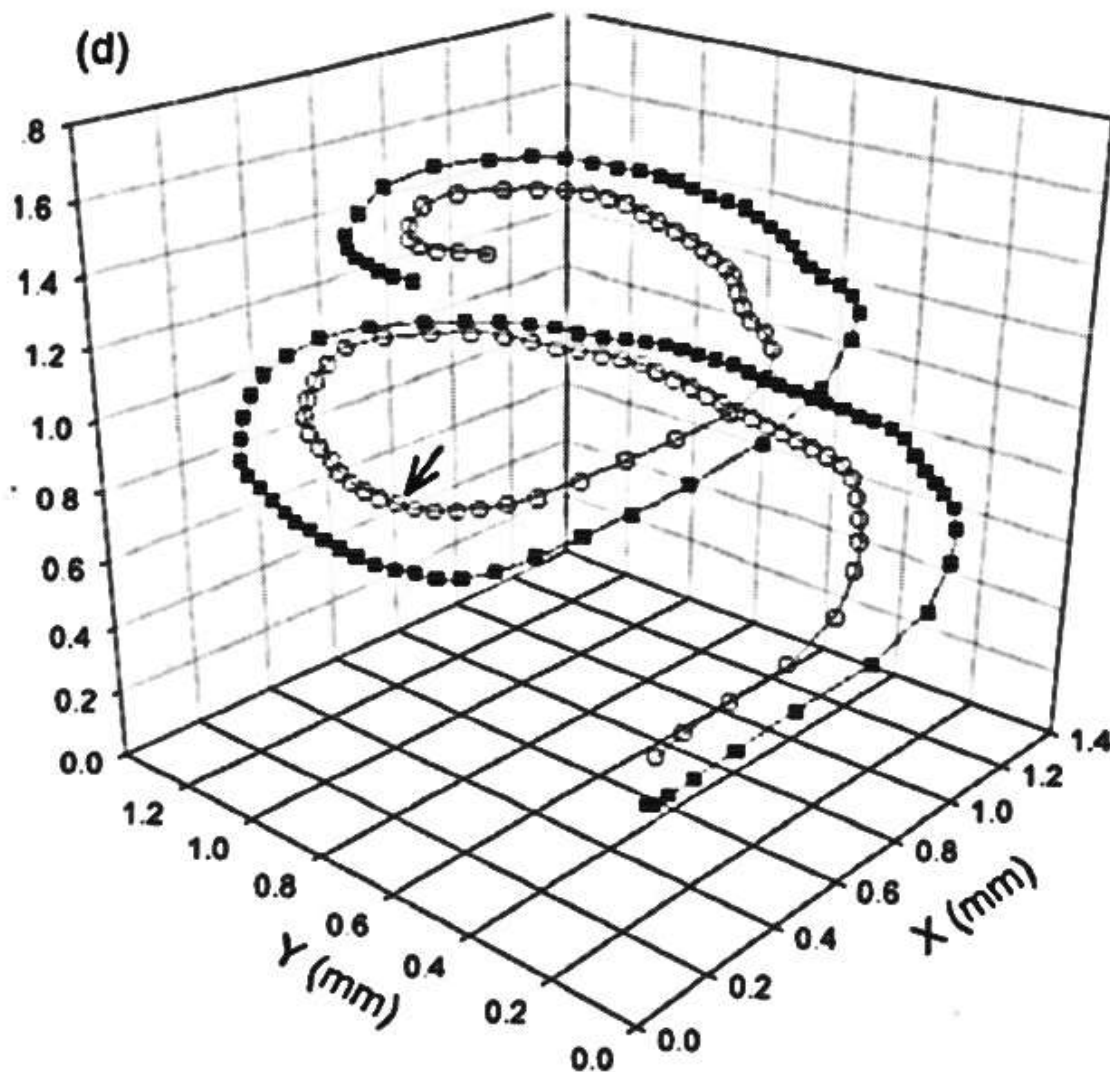
Figure 2. The basilar membrane (BM) in three dimensions in the CBA/J mouse cochlea. Filled and open (arrow) symbols represent anchoring points of the BM. Figure from (Müller et al., 2005).

In mammals the hearing organ is situated inside the cochlea which is located inside the petrous part of the temporal bone. In mice it consists of two turns in a spiral structure (Müller et al., 2005), as shown in Figure 2. Mice have a behavioral hearing range from 1 kHz to 100 kHz (Reynolds et al., 2010). High frequencies are detected at the base of the cochlea, whilst the lower ones at the apex. The oval window (ow) is the entry port of sound pressure waves from the middle ear into the fluid-filled cochlea. The cochlea is divided into three compartments (scalae), spiraling together throughout the entire cochlea's length (Figure 2 and 3).

These three compartments contain either perilymph or endolymph (Geisler, 1998). Scala tympani (ST), scala media (SM) and scala vestibuli (SV) are the three compartments essential for the transduction of sound pressure into electrochemical stimulation. Sound pressure arriving from the middle ear through the oval window sparks fluid movements in the 3 scalae. A non-

linear phenomenon called traveling wave builds up at the basilar membrane (BM), leading to displacements at a certain place of the BM. It provokes stimulation of hair cells and the transduction of sound pressure into mechanical, electrical, and chemical activation. The SM is completely isolated from the two other scalae by the Reissner's membrane on top, and the BM at the bottom.
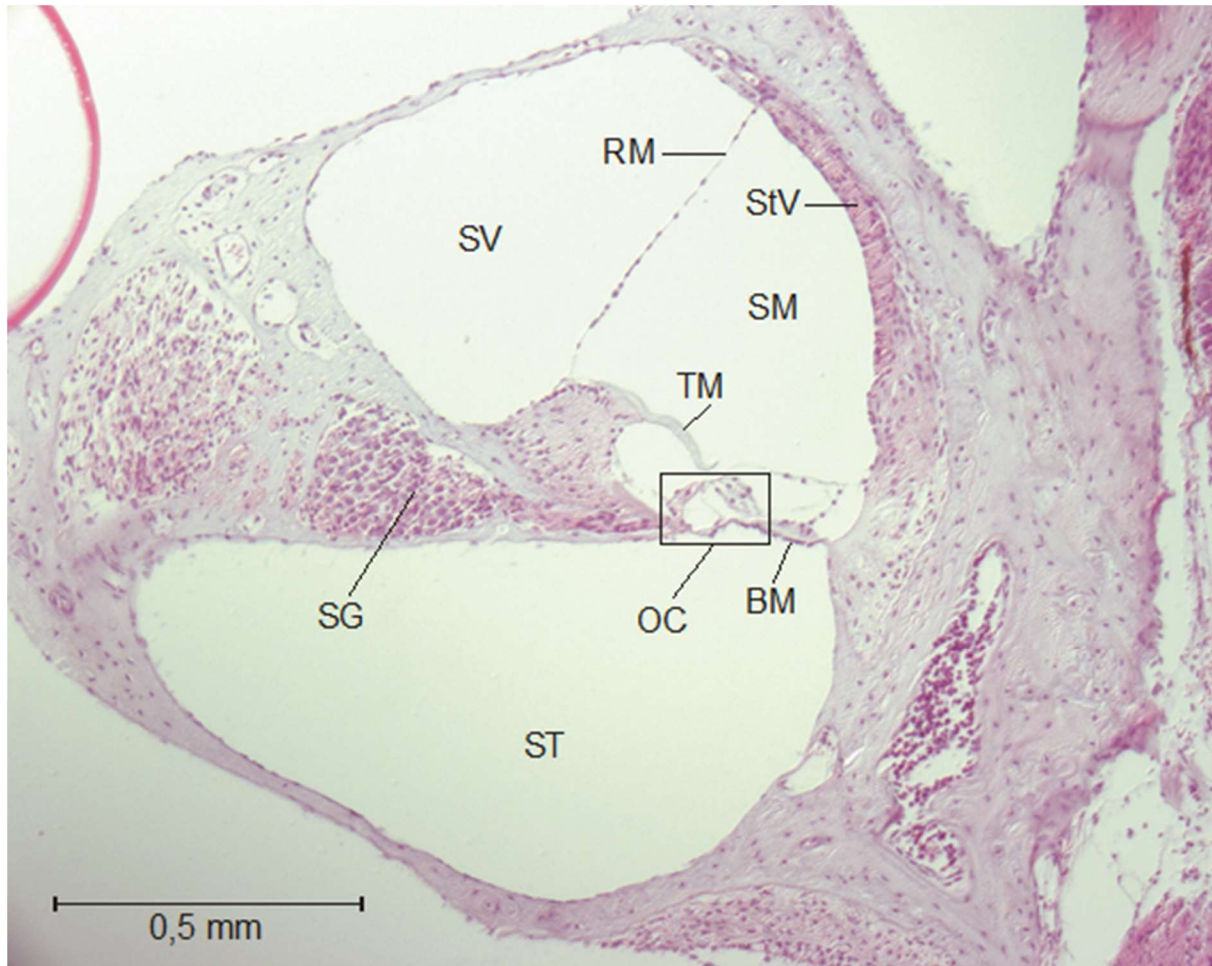
Figure 3. Cross section through the mouse cochlea. Three liquid-filled scalae are visible: scala vestibuli (SV), scala media (SM) and scala tympani (ST). The Organ of Corti (OC) is sitting on the basilar membrane (BM). Nerve fibers are leading to the spiral ganglion (SG). Tectorial membrane (TM), Reissner's membrane (RM) and stria vascularis (StV). Figure from (Kurt, 2001).
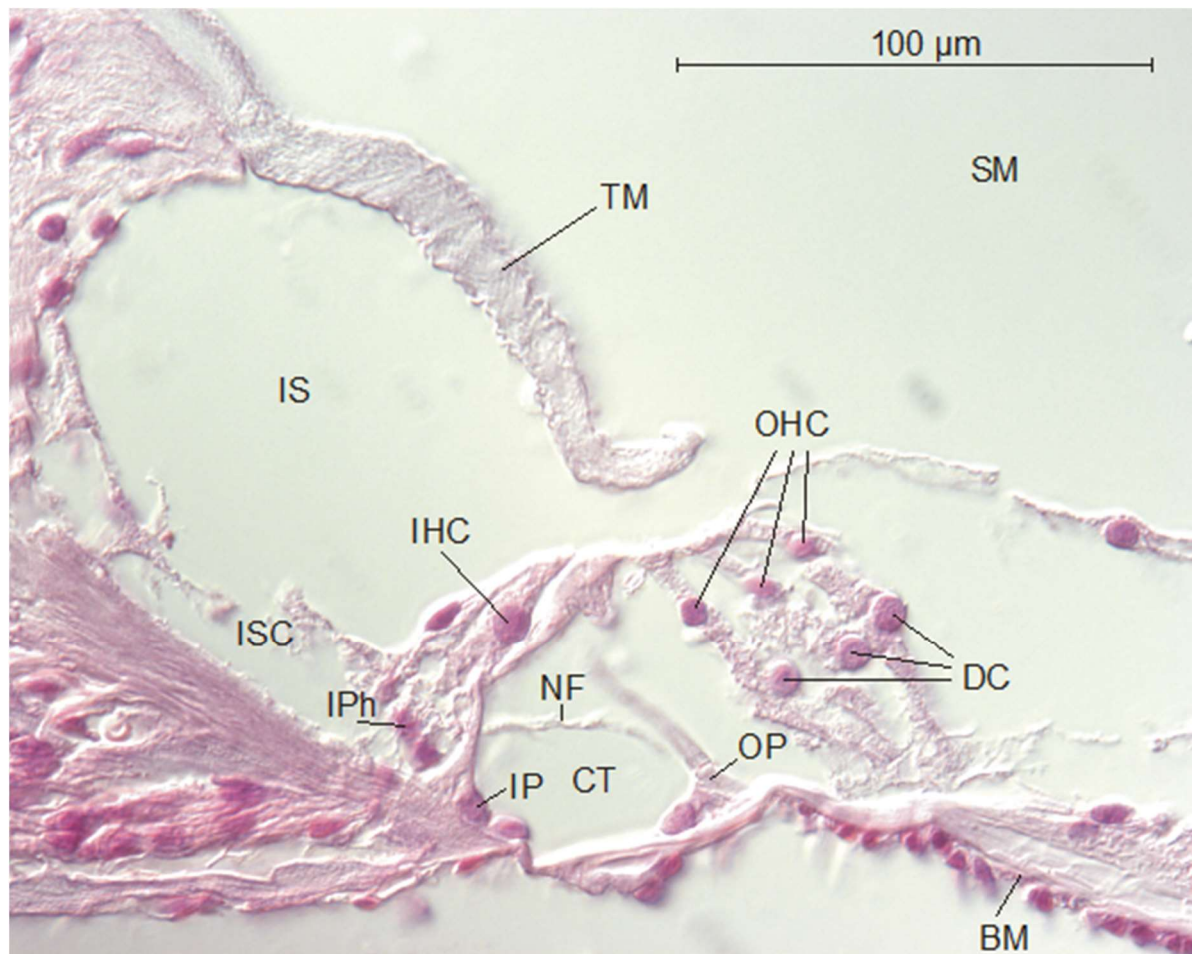
Figure 4. Murine Organ of Corti, radial section. Inner hair cells (IHC) with neighboring inner phalan-geal cells (IPh) facing outer hair cells (OHC) sitting on Deiter´s cells (DC). The tunnel of Corti (CT) is built of inner (IPC) and outer pillar cells (OPC), here crossed by nerve fibers (NF). The inner sulcus (IS) contains inner sulcus cells (ISC). The IS is separated from scala media (SM) by the tectorial membrane (TM). BM = basilar membrane. Figure from (Kurt, 2001).

The SM contains the sensory epithelium, the organ of Corti (Fig. 4). As an extracellular com-partment it is filled with a highly unusual electrochemical composition: a high concentration of potassium ions (~150 mM) combined with a highly positive potential (+85 mV). This endolymph surrounds the apical parts of the inner (IHC) and outer hair cells (OHC), as seen in Figure 4. Hair cells bear three rows of stereocilia of different height at their top. Stereocilia of different rows are interconnected with tip links (Fettiplace, 2017). At the lower insertion site of a tip link, mechano-transducing ion channels sit in the hair cell's membrane (Pickles, 2013), opening up when deflected towards the tallest stereocilia through sound-induced endolymph movement. Driven by a high potential difference between SM and hair cells, potassium ions flow into the negatively charged hair cells causing depolarization. The sensory hair cells transduce me-chanical energy into depolarizing electrochemical energy.

Fluid waves and BM movements are amplified by action from OHCs (Geisler, 1998). They improve both frequency tuning and frequency resolution. Sound-induced depolarizations of

OHCs cause extremely rapid contractions of OHCs via the piezoelectric motor protein prestin (Fettiplace, 2017). This motor activity facilitates mechanical activation of IHCs followed by depolarization, but simultaneously also produces sounds that exit the inner ear and middle ear and can be captured by very sensitive microphones in the external ear canal. They are called otoacoustic emissions (OAE). One particular example for OAEs are distortion product otoacoustic emission (DPOAE). This method is non-invasive and objective, can be performed in awake and anesthetized subjects, and provides a very reliable view of OHC function.

In each IHC, so-called ribbon synapses are connected to 10-20 afferent auditory nerve fibers, the peripheral dendrites of spiral ganglion (SG) neurons type I. Depolarization causes exocytosis of glutamate in these ribbon synapses. Ribbon synapses and afferent nerve fibers differ in threshold and spontaneous activity. There are high spontaneous rate (HSR) fibers with small dynamic range, low spontaneous rate (LSR) fibers with large dynamic range, and medium spontaneous rate (MSR) fibers with medium dynamic range. HSR fibers are thick and rich in mitochondria and contact the IHC on its pillar side. LSR and MSR fibers are thinner, have less mitochondria and contact the IHC on the modiolar side (Figure 5). Ribbon synapses and different afferent nerve fibers play an important role in synaptopathy and hidden hearing loss (Furman et al., 2013; Kujawa and Liberman, 2009; Suthakar and Liberman, 2021).
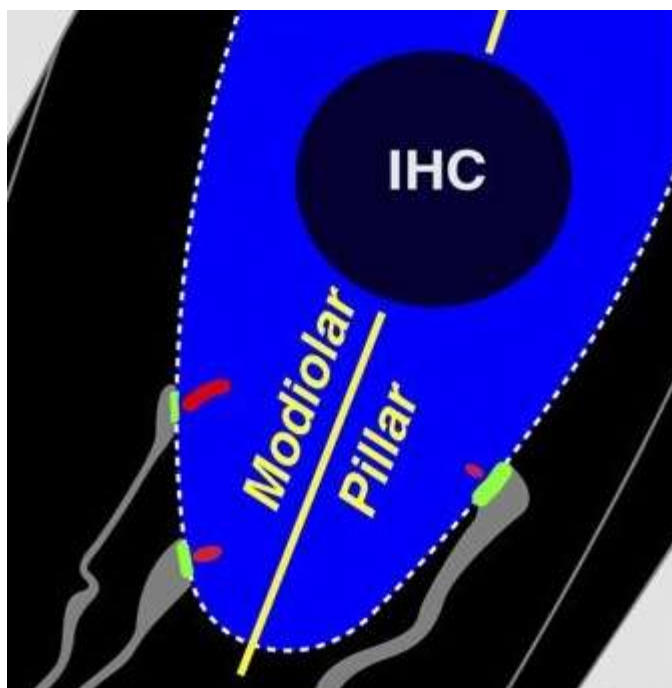
Figure 5. Inner hair cell and localization of three types of afferent nerves. Note different synapses and types of nerve fibers on modiolar and pillar side. The modiolar face of an IHC is directed to the center of the cochlea, the modiolus, whereas the pillar face is directed towards the pillar cells and the OHCs. Figure from (Furman et al., 2013).

Threshold sensitivity and auditory fiber distribution with high and low-spontaneous rate peripheral nerves have been confirmed in mice, rabbits, guinea pigs and gerbils (Borg et al., 1988; Furman et al., 2013; Liberman, 1978; Schmiedt, 1989; Tsuji and Liberman, 1997). This suggests that we are looking at a general principle in the mammalian auditory system. Recently, molecular analyses have confirmed the existence of three different type I auditory neurons – type Ia, Ib, and Ic (Petitpré et al., 2018; Shrestha et al., 2018; Sun et al., 2018), which correspond to neurons giving rise to high spontaneous rate (HSR), medium spontaneous rate (MSR) and low spontaneous rate (LSR) fibers.

The impact of noise exposure has been studied in several mammals with very similar physiological and histological reactions, for example in cats, guinea pigs and mice (Liberman, 1982; Pujol et al., 1993; Wang et al., 2002). A similar neural degeneration in noise-exposed human ears is considered highly probable by many authors (Kohrman et al., 2019; Kujawa and Liberman, 2009). However, conflicting and controversial studies may require a different methodological approach to acquire certainty (Bramhall et al., 2019).

3.2   Auditory brainstem responses (ABR)

3.2.1   ABR working principle

In this experiment, thresholds and hearing functions were measured with auditory brainstem response audiometry (ABR).

ABR is a non-invasive technique to portray the auditory pathway (Figure 6). It shows five typical waves, numbered in Roman letters I to V, that represent the successive excursions of the auditory neuro-electrical response to sound. It can be considered as the equivalent of a compound action potential (CAP). The wave peaks are positive when the active electrode is placed on the mouse´s vertex. In our study, the active electrode was placed behind the respective pinna, thus inverting polarity.
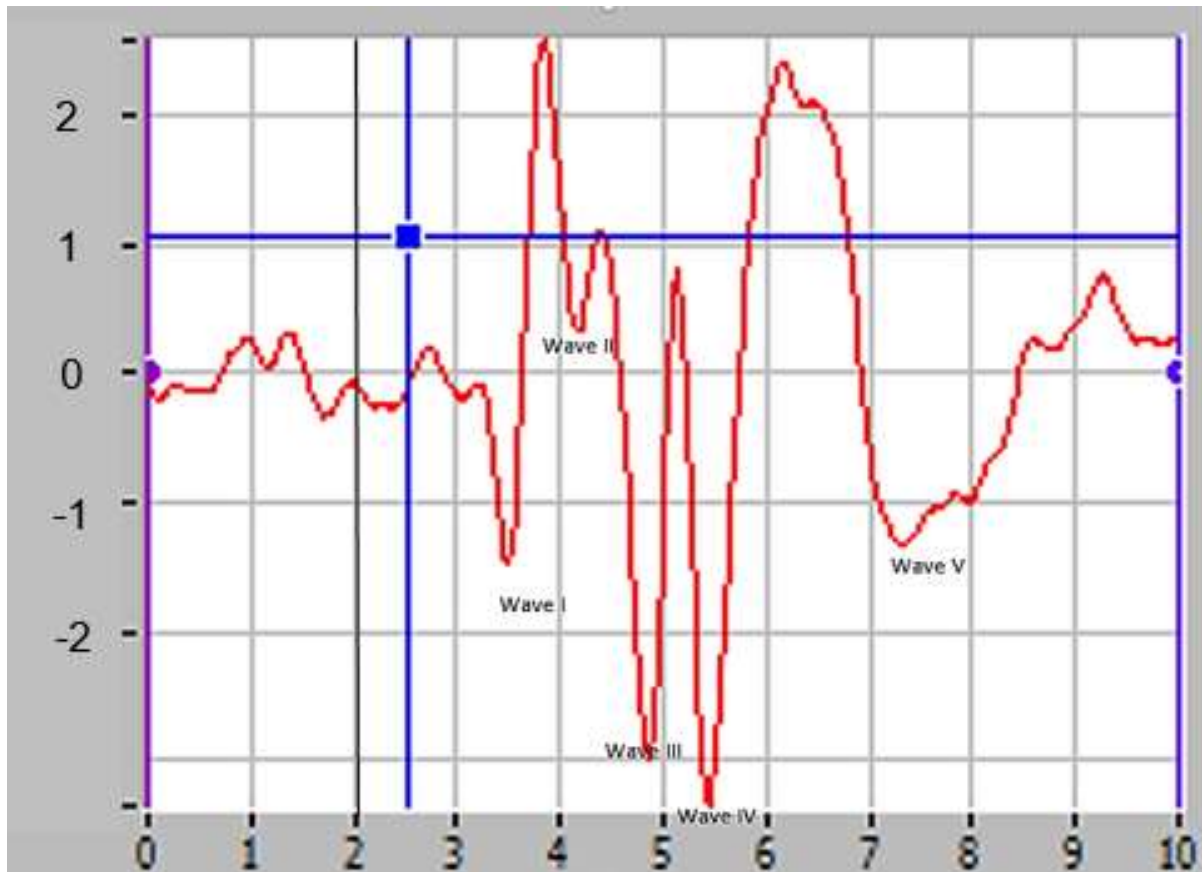
Figure 6. Typical click-induced ABR waves of a C57BL/6N mouse. The ordinate represents the ABR amplitude in µV, the abscissa the time in milliseconds. The click was delivered at 2 ms. Blue crosshair is a user's measurement tool.

Amplitudes of ABR waves are measured in µVolt from trough to the following peak. Waves in humans and mice represent similar yet slightly different stations of neuronal sound processing along the ascending auditory pathway. In mice, wave I represents the summed activity of the auditory nerve built by the axons of spiral ganglion neurons. Their afferent dendrites are in contact with IHC ribbon synapses. Wave II represents the cochlear nucleus, wave III the superior olivary complex (SOC), and wave IV the lateral lemniscus and inferior colliculus (IC). Wave V is considered IC output activity (Figure 7).
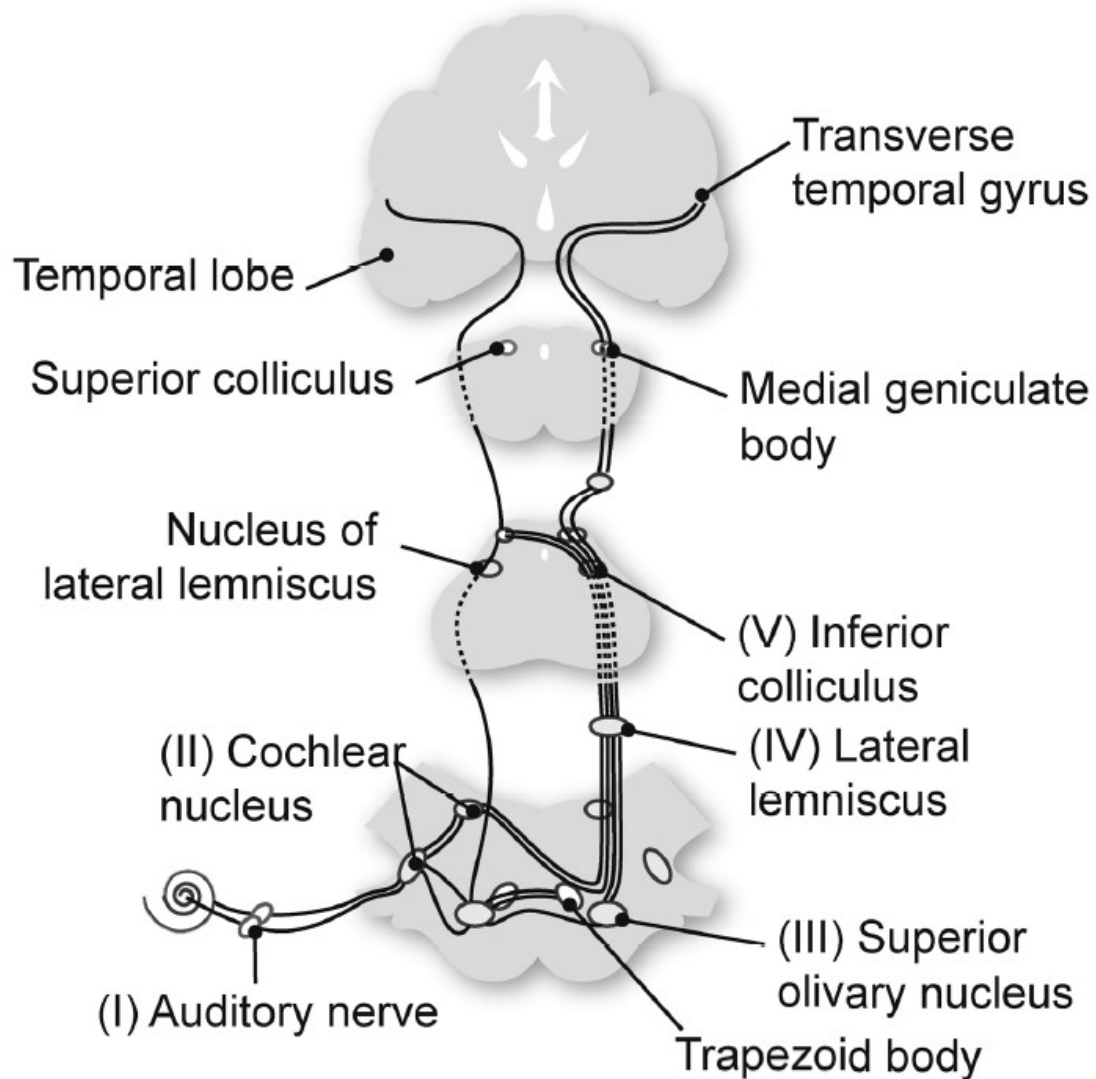
Figure 7. Scheme of the auditory pathway in mice and its anatomical counterparts. The origin of the particular waves of the auditory brainstem response are marked in Roman letters I to V. Figure from (Murillo-Cuesta et al., 2012).

3.2.2 ABR use in this study

ABR can be elicited by either click or pure tone stimulation, yielding e.g. click and pure tone thresholds. Elevation of thresholds is considered the most important indicator for hearing loss in clinical audiograms (Liberman and Kujawa, 2017; Lopes et al., 2009; NIOSH, 2012). If a conductive hearing loss can be excluded, it points to sensorineural hearing loss mostly caused by outer hair cell damage (Natarajan et al., 2023; Wang et al., 2002).

In addition, ABR can also be used to detect biomarkers for noise-induced hidden hearing loss (NIHHL), as described in chapter 3.3. These biomarkers consist of supra-threshold modifications of amplitudes and latencies, even with normal hearing thresholds.

NIHHL can diminish supra-threshold ABR amplitudes of wave I (Kujawa and Liberman, 2009; Rüttiger et al., 2017). Even with OHCs intact, part of the auditory fibers contacting IHCs may not function properly because of de-afferentation, e.g. through lost synapses or nerve degeneration (Trautwein et al., 1996).

Another biomarker in this respect is the peak latency of ABR waves, especially of wave I. Modified latencies of peaks, interpeaks or interwaves can be found in NIHHL (Gourévitch et al., 2009; Mehraei et al., 2016).

Coupling these physiological phenomena to histological findings (number of IHC ribbons, postsynapses, and their pairing) is the work of the fellow dissertation of cand. med. P.Schätzle (Blum et al., 2024; Schätzle, unpublished).

3.3 Noise trauma and cochlear synaptopathy

The field of hidden hearing loss and cochlear synaptopathy covering different noise exposure paradigms in mice, guinea pigs, non-human primates, and humans literally exploded in the past 15 years and produced many and partially contradicting results (Liu et al., 2024).

In a 2006 publication (Kujawa and Liberman, 2006), a 2-hour 100 dB noise exposure of a 8-16 kilohertz (kHz) octave band revealed permanent threshold shift (PTS) in addition to cell degeneration in spiral ganglion cells (SGC) and fibrocytes in CBA/CaJ mice, while DPOAEs returned to normal. Particularly younger mice (aged 4-8 weeks) were vulnerable, but even older mice suffered long term effects.

In a landmark experiment, CBA/CaJ mice aged 16 weeks were exposed to noise of 100 dB SPL for two hours, 8-16 kHz (Kujawa and Liberman, 2009). This exposure evoked only a temporary threshold shift (TTS) without loss of IHCs or OHCs. However, ribbon synapses between IHC and the cochlear afferent SGN dendrites in the high frequency region were found to be particularly vulnerable to trauma. On the histological level, paired immunolabeled puncta of pre- and postsynaptic protein clusters are considered to be coupled synapses. More than half of the ribbon presynapses were irreversibly lost in the 32 kHz region, and afferent dendrites were reduced as well. Synaptic destruction began within a few hours and lasted for months, with possible SGN destruction occurring afterwards.

Because regularly tested hearing thresholds returned to normal, a new phenomenon was detected: noise-induced hidden hearing loss (NIHHL). A similar phenomenon was discovered in aging mice without noise trauma (Sergeyenko et al., 2013). Hidden hearing loss can be diagnosed by normal hearing thresholds and a reduction of the amplitude of ABR wave I in the high frequency region. In humans, hidden hearing loss (HHL) may underlie tinnitus, hyperacusis and difficulties understanding speech in noisy environments (Anderson et al., 2018; Kohrman

et al., 2019; Schaette and McAlpine, 2011). In CBA/CaJ mice, a reduction of the number of functional auditory nerve fibers was discovered, which affected mainly those with high-threshold, low spontaneous rate synapses. They are predominantly located on the modiolar side of the IHC (Furman et al., 2013; Liberman and Kujawa, 2017; Song et al., 2016). Low-threshold, high spontaneous rate synapses on the pillar side of the IHC were still active and apparently responsible for maintaining normal hearing thresholds. A recent study has displayed even more complex changes in high and low-threshold fibers in CBA/CaJ mice after noise trauma (Suthakar and Liberman, 2021). For example, a paradoxical gain-of-function in surviving low-threshold fibers was found, suggesting a hyperexcitability in the central auditory circuits including the auditory nerve. In other mouse lines such as C57BL/6 and in guinea pigs, evidence for regeneration of part of the ribbons and entire synapses was found after a TTS trauma (Chen et al., 2018; Kaur et al., 2019).

Differences between mouse strains in hearing performance and in the vulnerability towards noise trauma have been described (Boussaty et al., 2020; Ohlemiller, 2019; Reijntjes et al., 2020; Zhou et al., 2006). C57BL/6J are more vulnerable to age-related and noise-related hearing loss (Davis et al., 2003) than, for example, CBA/CaJ. Presbycusis in C57BL/6J can start as early as six months of age (Chen et al., 2012; Jackson Laboratories, n.d.). Mice in our experiment were selected at a far earlier stage, between seven and eight weeks of age.

Auditory experiments are technically and ethically difficult to conduct on humans. Using animal studies to predict human auditory functions after noise trauma can be disputed. Studies are often laborious to compare, using different parameters and settings (Bramhall et al., 2019), and the results can be contradictory.

The Occupational Safety and Health Administration (OSHA) in the United States sets a legal limit to workplace noise exposures ("CDC - Noise and Hearing Loss Prevention - Reducing Noise Exposure, Guidance and Regulations - NIOSH Workplace Safety and Health Topic," 2018). Sound exposure to 100 dB SPL is allowed on a daily two-hour basis. For preserving hearing health, this limit is probably too high. All experimental findings using mice as model animals should be viewed from a "human" perspective.

3.4   Aim of this thesis

This thesis can be considered as a follow-up study of the medical thesis of Fahmi Nasri who exposed C57BL/6N mice to the classical hidden hearing loss noise trauma (100 dB SPL from 8 - 16 kHz for 2 h) (Kujawa and Liberman, 2009) in our laboratory (Nasri, 2023). The aim of the present thesis was to analyze the effects of two more intense noise traumata of 106 and

112 decibel sound pressure level (dB SPL), respectively, on hearing thresholds and auditory functions by means of auditory brainstem response (ABR) measurements in C57BL/6N mice. A fellow medical thesis by Philipp Schätzle in the same department of Biophysics examined the histological fate of OHCs, presynapses, postsynapses, and synaptic pairing as a function of trauma by using immunofluorescence and high-resolution laser scanning microscopy (Schätzle, unpublished). This work was carried out on a subset of the mice of the present study and in correlation with temporary or permanent threshold shifts analyzed here.

The aims of this thesis are to answer the following questions:

1. How does the trauma strength (106 dB SPL, 112 dB SPL) scale with temporary and with permanent threshold shifts in click-ABR and in f-ABR stimulation?
2. What are the effects of either trauma on the peak latencies and amplitudes of click-ABR waves I – V up to four weeks after trauma?
3. How does either trauma affect the amplitudes of growth functions of click-ABR wave I two and four weeks after trauma?
4. How does the 106 dB SPL trauma affect the amplitudes of f-ABR wave I growth functions in the medium to high frequency range four weeks after trauma?

Here, the C57BL/6N mouse line was used, which has been very popular for generating genetic mouse models (knock-in and knock-out mice) in basic research (Mianné et al., 2016).

4 Material and methods

4.1 Animals

All experiments were authorized by the Animal Welfare Commissioner and the Regional Board of Animal Experimentation of Saarland at the Ministerium für Umwelt und Verbraucherschutz (License 17/2017). They were performed in accordance with the European Communities Council Directive (86/609/EEC). Mice came exclusively from the C57BL/6N strain, both sexes. They weighed between 14.9-30.1 grams throughout this study. They were bred and raised in our own university facility. Mice were between 46 and 64 days old at the beginning of the experiments. Groups were randomly and evenly composed regarding sex and age distribution, with 8 female and 16 male mice. The 106 dB and 112 dB noise trauma groups had 10 mice each, the control group 4 mice. This thesis refers frequently to a 100 dB SPL noise trauma group (Nasri, 2023), containing 8 mice. Procedural parameters were exactly the same in Nasri's experiments, except for the mice's age at the beginning of experiments: 74 to 84 days. Advantage from inbred mouse strains in a laboratory setting is a diminished variability in their physiological reactions to noise-induced hearing loss (NIHL). Outbred animals show a larger panel of reactions (Yoshida et al., 2000).

Our mice were kept in a temperature-controlled facility (21°-23° Celsius) with a light-dark cycle of 12 hours. Humidity was at around 55%. Food and water were available at all time.

4.2 Anesthesia

Noise exposure and measurement of auditory brainstem response (ABR) were conducted under anesthesia. Anesthetics were injected intraperitoneally, antidotes subcutaneously. Narcotics dosage was a mixture of 0.05 mg/kg Fentanyl (Fentanyl-hameln® 50 microgram/ml, Hameln Pharma Plus GmbH, Hameln, Germany), 5 mg/kg of Midazolam (Midazolam-hameln® 5 mg/ml, Hameln Pharma Plus GmbH, Hameln, Germany) and 0.5 mg/kg and of Medetomidin (Domitor® 1 mg/ml, Orion Corporation, Espoo, Finland). Surgical tolerance was obtained after 15 minutes of injection for approximately 75 minutes. One third of the initial dose of anesthetics was added if necessary. Toe pinch reflexes through stimulation were tested about every 40 minutes.

The antidotes' dosage was a mixture of 1.2 mg/kg Naloxon (Naloxon Inresa® 0.4 mg, Inresa Arzneimittel GmbH, Freiburg, Germany), of 0.5 mg/kg Flumazenil (Flumazenil Inresa® 0.5 mg i.v., Inresa Arzneimittel GmbH, Freiburg, Germany) and of 2.5 mg/kg Atipamezol (Antisedan® 5 mg/ml, Orion Corporation, Espoo, Finland). The antidote was injected immediately after the end of each ABR experiment to shorten the duration of anesthesia. During anesthesia the mice were kept warm on a heating pad at approximately 37 degrees Celsius.

Ointment (Bepanthen® Augen- und Nasensalbe, Bayer Vital, Leverkusen, Germany) was applied on the mouse's eyes to prevent dryness.

4.3 Experimental procedures

Devices

The auditory stimulation and recording system (Audiology_Lab, Otoconsult, Marcus Müller, Frankfurt/Main, Germany) was conceived to generate tones of a desired level and frequency and simultaneously record incoming ABR signals. A personal computer was equipped with a National Instruments data acquisition card (National Instruments, Austin, USA) and custom-made software. The National Instruments data acquisition card offered 16 bit resolution at adequate sampling rates for AD and DA conversion. The software was written in LabWindowsCVI, a software development suite from National-Instruments for the programming language "C/C++". Averaged recorded potentials were stored in ASCII format and were analyzed later. The computer was able to generate and calibrate acoustic stimuli and simultaneously register ABR signals from the animal evoked by the acoustic stimuli. ABR signals were amplified and filtered before recording.

All experiments were conducted in a sound-attenuated chamber and animals were placed on a heating pad during the experiment.

Noise trauma exposure

A tweeter horn (MHD-220N/RD, Monacor®, Bremen, Germany) was placed in the middle of the lid of the sound attenuation chamber right above the animal's ear at a distance of approximately 30 cm.

Before the experiment, calibration of the speaker was performed with devices from Brüel & Kjaer, Naerum, Denmark. The microphone B&K 4135 was placed at the same place as the animal's ears in the experiment. The measuring amplifier B&K 2636 was used. A frequency analysis was performed using the Ono Sokki Multipurpose FFT Analyzer CF-5220, Ono Sokki Technology, Yokohama, Japan).

The noise trauma generator was part of Audiology_Lab (Otoconsult, Marcus Müller, Frankfurt/Main, Germany). Noise trauma was an octave band of 8-16 kHz which lasted for two hours, with two different sound pressure levels. A first group (10 mice) was exposed to 106 dB SPL, a second group (10 mice) to 112 dB SPL. The higher trauma strength corresponds to a doubling of sound pressure level of the lower trauma.

A control group (4 mice) was neither exposed to noise, nor to a sham procedure.

All mice underwent ABR measurements of both ears and were sacrificed by cervical disloca-tion on day 28. A histological examination (thesis of cand. med. P.Schätzle) was performed on a sample of all groups.

Acoustic stimuli and ABR parameters

Hearing thresholds, wave peak amplitudes and latencies were measured on days -2 (before noise trauma), 0 (immediately after noise trauma), 1, 3, 5, 7, 14, 21 and 28 after trauma in both noise exposure groups (Figure 8). Control group was measured only on day 0 and 28.

Timeline of experiments
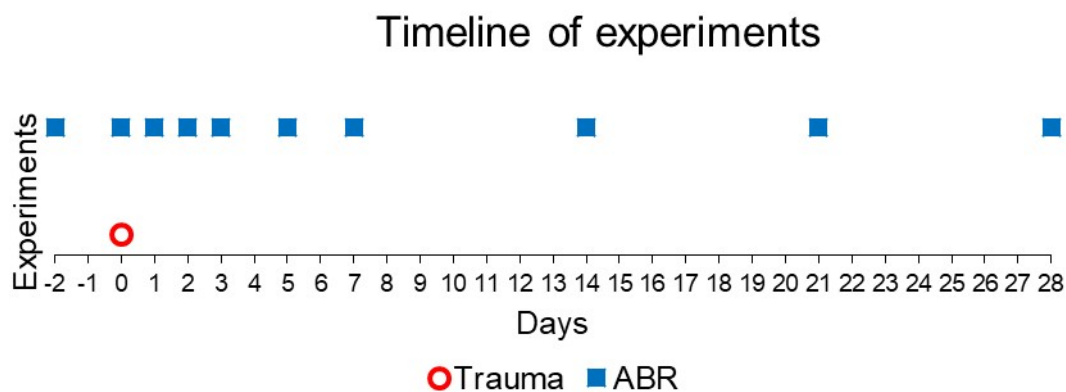
Figure 8. Timeline of noise trauma experiments. Blue squares show the days of ABR measurements, the red circle shows the day of noise trauma. The control group was measured on day 0 and on day 28.

Electrodes were placed subcutaneously on the vertex (reference electrode), respective pinna (active electrode) and in the dorsal tail area (ground). ABR from both ears were measured in every session.

Stimuli, either click or pure tone, were presented at a frequency of 80/sec from a loudspeaker placed 2 cm from the mouse's head. A microphone was positioned in a 45° angle at 1 cm from the respective pinna (KE 4-211-2, Sennheiser, Wedemark, Germany) (Fig. 9).

Total duration of an ABR recording was around 45 minutes per mouse for both ears. ABR signals were recorded for 10 milliseconds (ms), whereas acoustic stimuli had a maximum du-ration of 3 ms including rise and fall time.
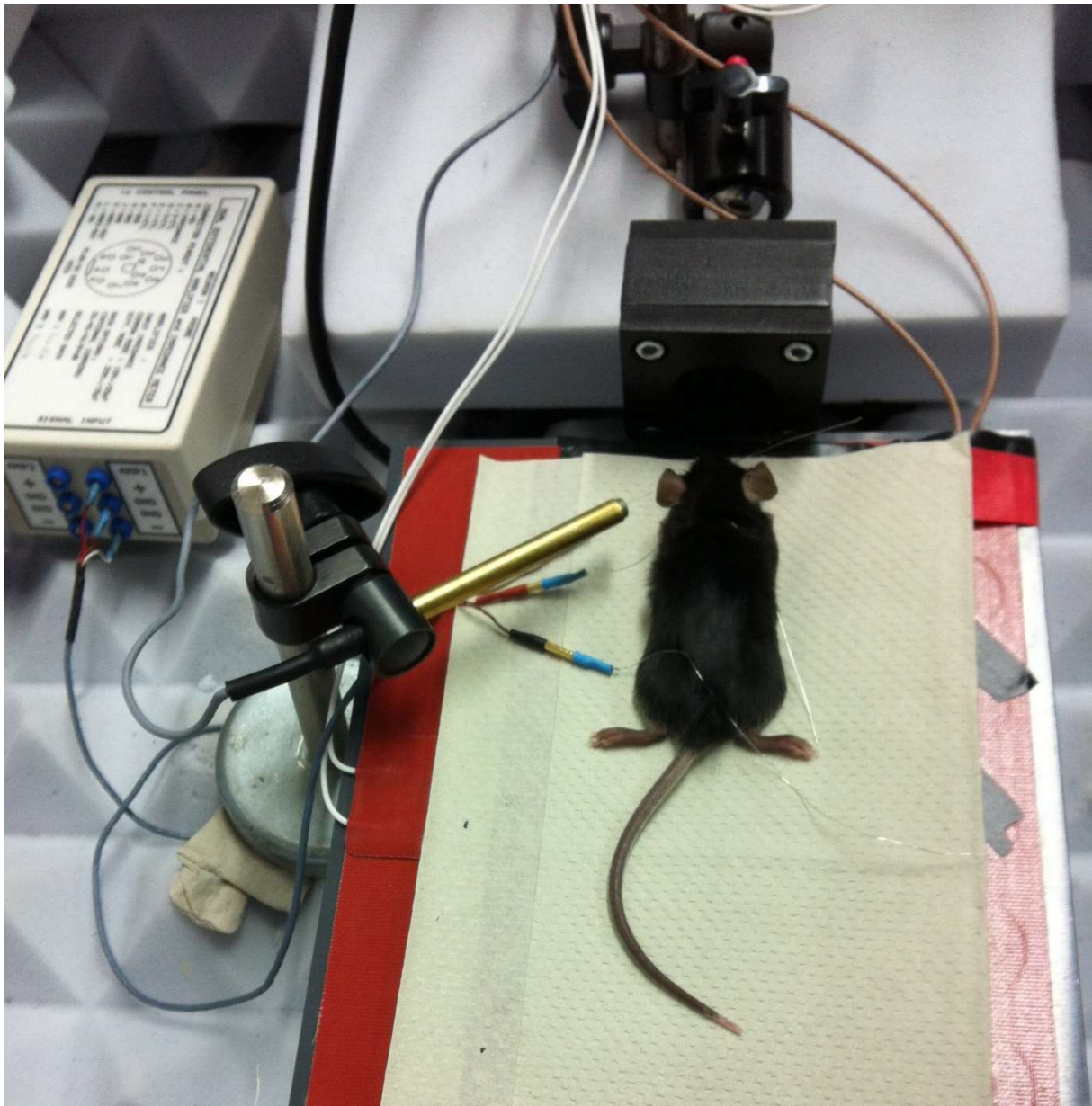
Figure 9. ABR recording of the mouse in the laboratory. The anesthetized mouse is facing the loudspeaker with subdermal electrodes inserted at vertex, behind the respective pinna and at the dorsal back. The animal is located on a heating pad and a microphone was used to calibrate the sound pressure level of the tones.

1. Acoustic stimuli

Click stimuli were used to determine gross thresholds. Clicks, which consist of a very large frequency range, of 100 µsec duration were presented in 5 dB SPL steps.

Each decibel step was situated in an attenuation range below the maximum possible sound pressure level that could be generated by audiology_lab (Otoconsult, Marcus Müller, Frankfurt/Main, Germany). It corresponded to sound pressure levels between 0 and 80 dB SPL. Click measurements did not require calibration.

Pure tones ranging from 2 to 45.2 kHz were presented in half-octave steps. They were generated at sound pressure levels between 0 to 100 dB SPL, in 5 dB steps. The total duration was 3 ms, including 1 ms rise and fall time in sine function (Fig.10).

Pure tones were amplified (Otoconsult, Marcus Müller, Frankfurt/Main, Germany) and then registered with a microphone (KE 4-211-2, Sennheiser, Wedemark, Germany) with a sensitivity of 127 mV/Pa throughout the ABR frequency range.

2. ABR signals were amplified by factor 1000 (60 dB), bandpass--filtered to preserve frequencies between 300-3000 Hz, then again amplified by factor 100 (40 dB). An analog-to-digital converter transformed the signal and displayed it on oscilloscope (Rigol DS 1054®, Rigol Technologies, Beijing, China). Signals were averaged over 256 repetitions in inverting modes, which eliminates artefacts and displays a better averaged ABR waveform. Amplified signals over 0.9 V and under -0.9 V were excluded, possibly generated by muscle artefacts or cardiac potentials. This corresponds to respective ABR voltages over 9 µV and under -9 µV before amplification.

Thresholds were determined as the lowest SPL that produced the characteristic waveform of the ABR potentials which could be visually differentiated from the noise level (Akil et al., 2016; Knipper et al., 2000; Kurt et al., 2009).

Recorded data were stored for later analysis. Peak-to-trough amplitudes and latencies were calculated using Microsoft Excel.

Figure 11 shows a simplified scheme of the setup.
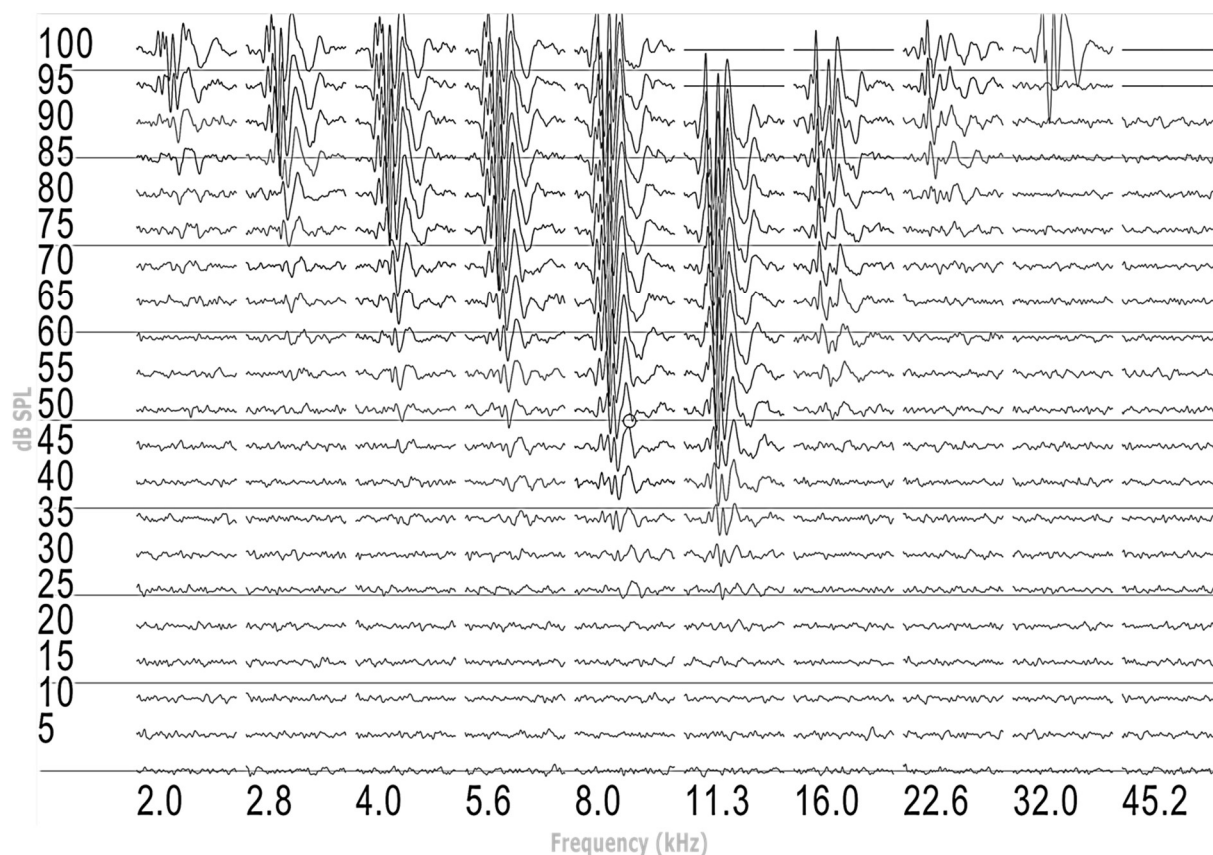
Figure 10. Frequency-ABR. Averaged extracranial potentials recorded in the first 10 ms after a pure tone stimulation is shown for increasing stimulus levels (y-axis, in dB SPL) as a function of stimulus frequency (x-axis, in kHz). Hearing thresholds were determined by the characteristic waveform of the ABR potentials which could be visually distinguished from the background noise.
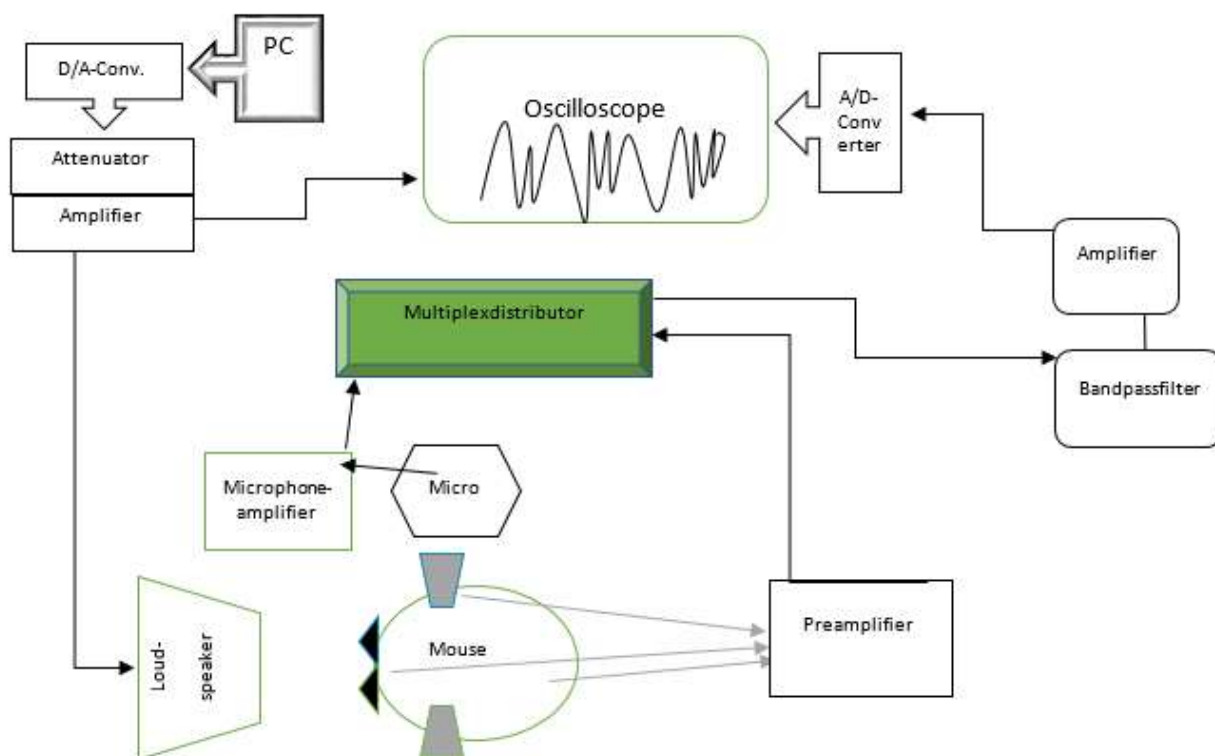
Figure 11. Simplified scheme of the ABR setup

4.4 Statistical methods

For threshold evaluation, an arbitrary threshold of 105 dB SPL was assigned whenever the measuring program "audiology_lab" was unable to produce a result (Fig. 12). This caused higher real thresholds than were detectable with "audiology_lab".
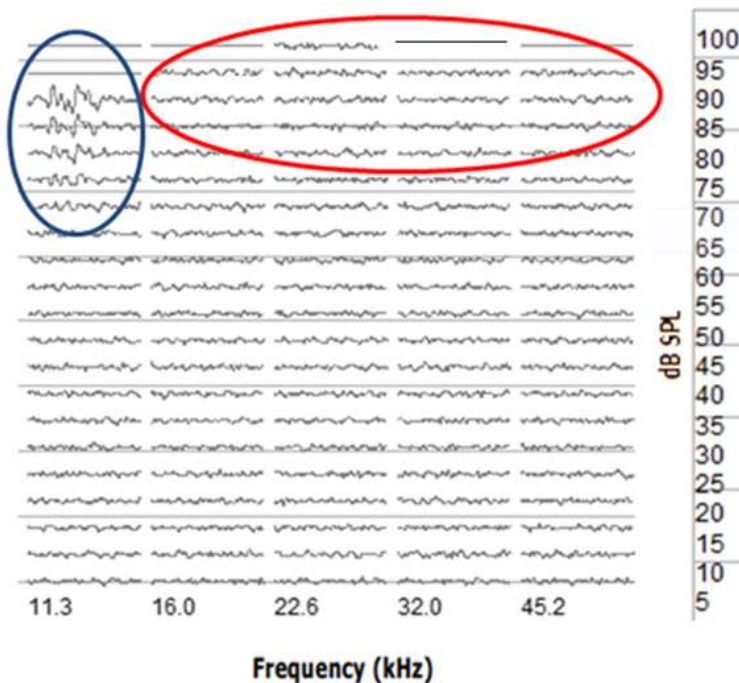
Figure 12. Example of a frequency-ABR and evaluation of thresholds. At 11.3 kHz, a threshold of 70 dB SPL was determined (blue ellipse) whereas arbitrary thresholds of 105 dB SPL were assigned to the frequencies from 16 to 45.2 kHz (red ellipse).

Data were used for calculation of group arithmetic means and standard deviations. Significant differences were analyzed through statistical tests (SPSS®, IBM, Armonk, USA) including threshold data of click and pure tone ABRs, supra-threshold amplitudes and latencies. Wilcoxon signed test, Friedman/Bonferroni test, Kruskal-Wallis/Bonferroni test and Mann-Whitney-U-test were used as described in the figures in the result chapter.

Asterisks were used in diagrams to give an immediate information of statistical significant differences.

5 Results

5.1 Hearing thresholds of click ABR recordings before and after trauma

Hearing thresholds in response to stimulation with either clicks or pure tones are the most common parameters to evaluate hearing impairment (Liberman and Kujawa, 2017), because they reveal underlying hair cell loss.
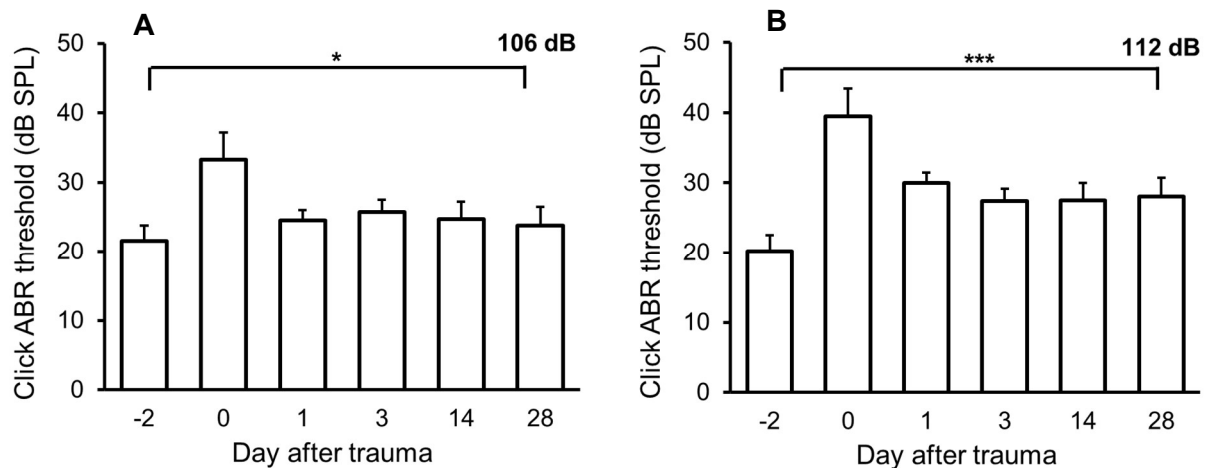
Figure 13. Time course of click thresholds of the 106 dB SPL (A) and 112 dB SPL (B) noise trauma groups. N = 20 ears each, except n = 18 ears for day 28 in figure B. Wilcoxon signed test, *p*-value 0.013 for A, < 0.001 for B when comparing pre-trauma and day 28 (asterisk).

Click-ABR thresholds increased significantly between pre-trauma day -2 and day 28 for both trauma groups (Fig. 13), and a higher trauma translated into a larger threshold shift. Whereas the 106 dB SPL trauma group showed a mean increase of the hearing threshold by 2.25 dB (from a mean threshold of 21.5 to 23.75 dB SPL) the 112 dB SPL trauma group displayed a mean increase of the hearing threshold by 7.81 dB (from 20.25 to 28.06 dB SPL).

5.2 Frequency-specific hearing thresholds before and after trauma

5.2.1 Frequency-specific thresholds

In the following chapter, hearing thresholds determined from responses to frequency-specific stimulation (frequency-specific ABR or f-ABR) are shown. Figure 14 summarizes f-ABR thresholds for the 106 dB SPL noise trauma group for the situation before (day -2), right after (day 0) and 4 weeks after trauma (day 28). There were significant differences (Wilcoxon signed test) between pre-trauma (day -2) and day 28 in the frequency range from 11.3 to 45.2 kHz (asterisks). The maximum threshold shift between day -2 and day 28 amounted to 30.8 dB at 22.6 kHz. This confirms and extends the results of a previous 100 dB SPL trauma experiment

(Nasri, 2023) in our department and validates a permanent threshold shift (PTS). A statistical analysis of f-ABR thresholds including all three days using the Friedman/Bonferroni test revealed significant frequency-specific differences in the lower frequency range as well. This was primarily due to threshold increases at day 0 (immediate post-trauma measurement).
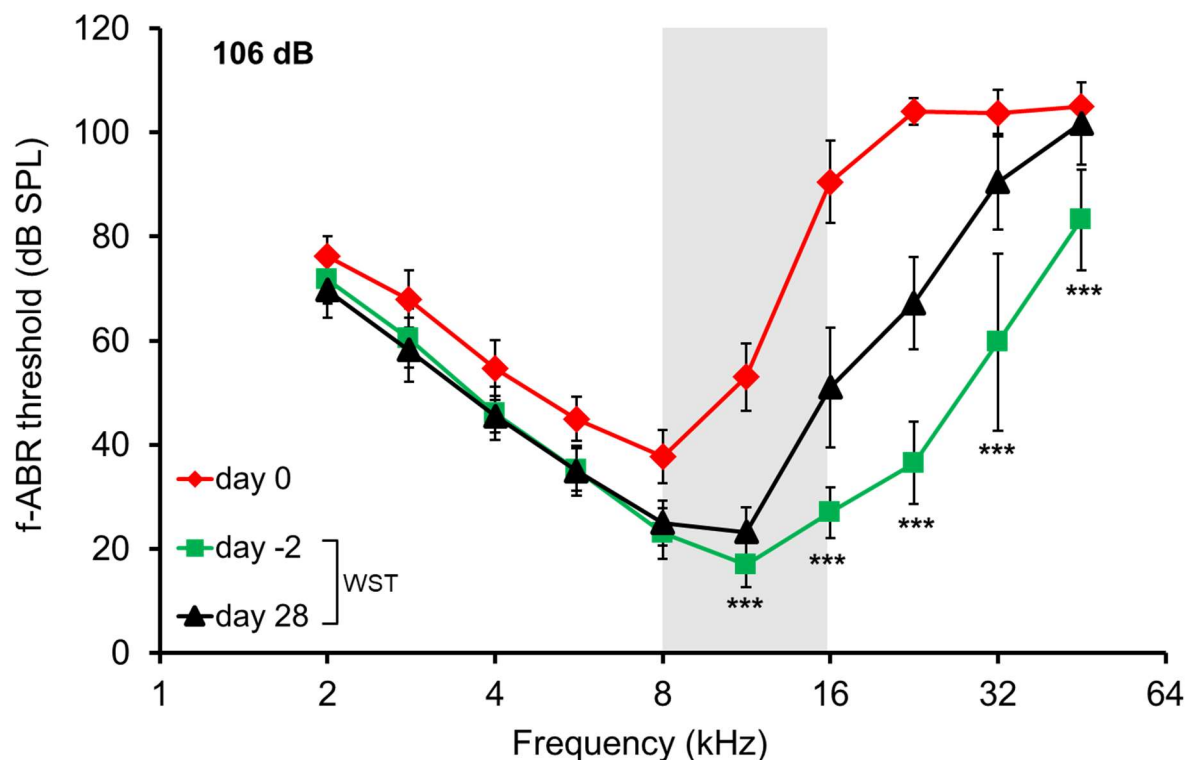
Figure 14. Effects of a 106 dB SPL noise trauma on frequency-ABR thresholds. Mean f-ABR thresholds ± standard deviation (SD) are shown before (day -2), directly after (day 0) and 4 weeks (day 28) after trauma, n = 20 ears. Significant differences (asterisks) between day -2 and day 28 (Wilcoxon signed test, WST) were present at 11.3 kHz ($p = 0.001$), 16 kHz ($p < 0.001$), 22.6 ($p < 0.001$), 32 kHz ($p < 0.001$) and 45.2 kHz ($p < 0.001$). Red graph (day 0) for information. The light grey bar reflects the trauma octave band.

Next, frequency-ABR thresholds of the experiments with a 112 dB SPL trauma are presented. F-ABR thresholds of the 112 dB SPL noise trauma group (Figure 15) showed significant differences between pre-trauma (day -2) and day 28 for all frequencies, except at 2.8 kHz (Wilcoxon signed test). The threshold shift peaked at 41.81 dB, shown at 22.6 kHz. There were also significant differences for all three days shown through the Friedman/Bonferroni test. A complete overview of thresholds of all days tested in the 106 and 112 dB SPL trauma groups is found in Chapter 8 (Figure 32-33).
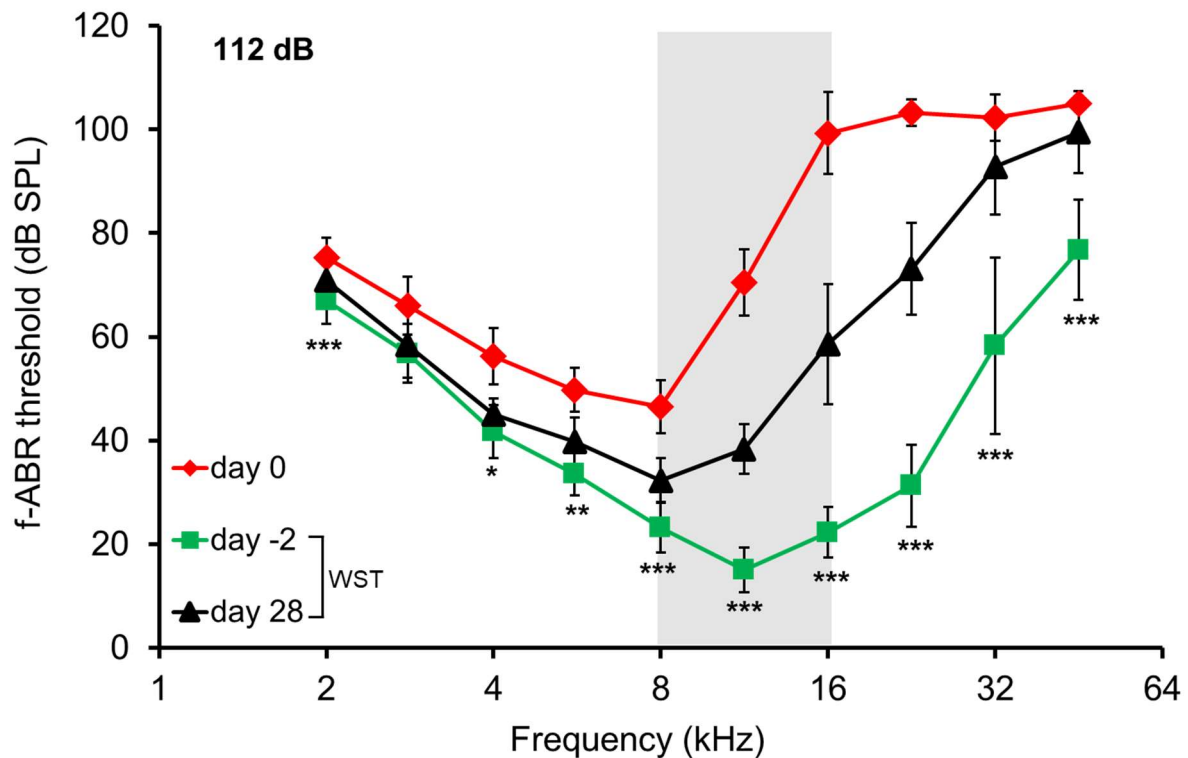
Figure 15. Effects of a 112 dB SPL noise trauma on frequency-ABR thresholds. Mean f-ABR thresholds ± SD are shown before (day -2), directly after (day 0) and 4 weeks (day 28) after trauma, n = 20 ears, except n = 18 ears on day 28. Significant differences between day -2 (pre-trauma) and day 28 for all frequencies (Wilcoxon signed test = WST) except 2.8 kHz. Table 1 specifies the *p-values*. Red graph for information. The light grey bar reflects the trauma octave band.

Table 1. Statistical analysis of the effects of the 112 dB SPL trauma on f-ABR thresholds on days -2 and 28. The *p*-values of the Wilcoxon signed test, n = 20 ears, except n = 18 on day 28, see Fig. 15.

	2 kHz	4 kHz	5.6 kHz	8 kHz	11.3 kHz	16 kHz	22.6 kHz	32 kHz	45.2 kHz
p-value	0.001	0.044	0.002	0.001	≤0.001	≤0.001	≤0.001	≤0.001	≤0.001

Figure 16 shows f-ABR thresholds of the three different trauma groups and a control group in the same diagram on day -2. In this pre-trauma situation, there were no significant threshold differences (Kruskal-Wallis/Bonferroni test) between groups at mid- to high frequencies starting from 5.6 kHz, with a single exception at 11.3 kHz. In spite of differences between some pairs, hearing functions were very similar in all groups.
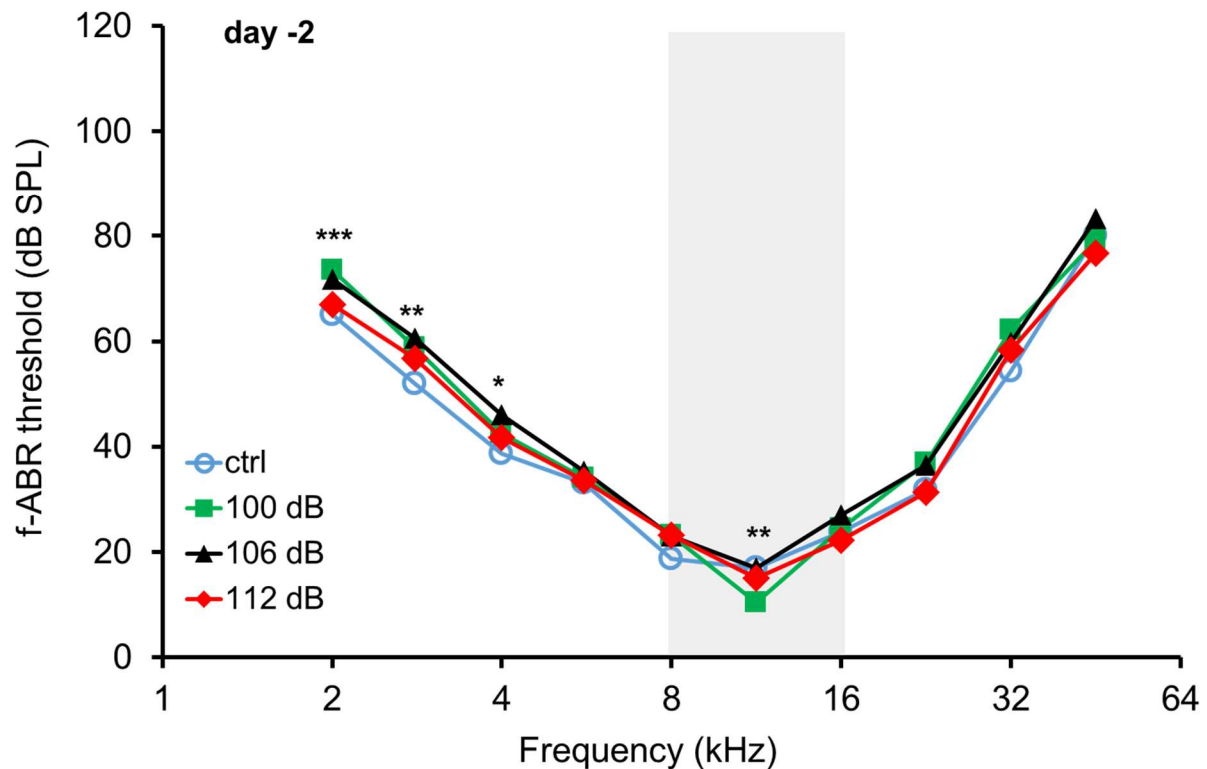
Figure 16. Initial frequency-specific hearing thresholds of three different trauma groups and a control group on day -2. N = 20 ears for 106 dB SPL, n = 20 for 112 dB SPL, n = 16 for 100 dB SPL (Nasri, 2023), n = 8 for the control group. For clarity, standard deviations are not shown. The Kruskal-Wallis/Bonferroni test revealed significant differences at 2 kHz ($p < 0.001$), 2.8 kHz ($p = 0.003$), 4 kHz ($p = 0.016$), 11.3 kHz ($p = 0.004$). An analysis of frequencies with significant differences are shown in Table 2. The light grey bar reflects the octave band of the trauma that was applied later.

Table 2. Statistical analysis of the initial f-ABR thresholds on day -2. The *p*-values of a detailed pair analysis of the Kruskal-Wallis/Bonferroni test of the initial hearing thresholds shown in Figure 16 where n-numbers for the tests are listed as well. Ns = not significant.

pair f (kHz)	ctrl	100	ctrl	106	ctrl	112	100	106	100	112	106	112
2	0.006		0.033		ns		ns		0.004		0.036	
2.8	0.036		0.002		ns		ns		ns		ns	
4	ns		0.021		ns		ns		ns		ns	
11.3	ns		ns		ns		0.004		ns		ns	

Figure 17 shows f-ABR thresholds on day 28, the end of the experiment, and thus reflects the PTS for each trauma group. Widened gaps are visible between the f-ABR threshold curves of all groups at the frequencies from 5.6 to 45.2 kHz (except for 32 kHz). Because of arbitrary thresholds of 105 dB SPL widely assigned to all groups at 32 and 45 kHz, the diagram shows

an artificial alignment between groups for the two highest frequencies. Actual thresholds lie probably much higher, especially for the more severe traumata. The diagram reveals that the intensity of the PTS is linked to the intensity of the trauma, which is coherent.
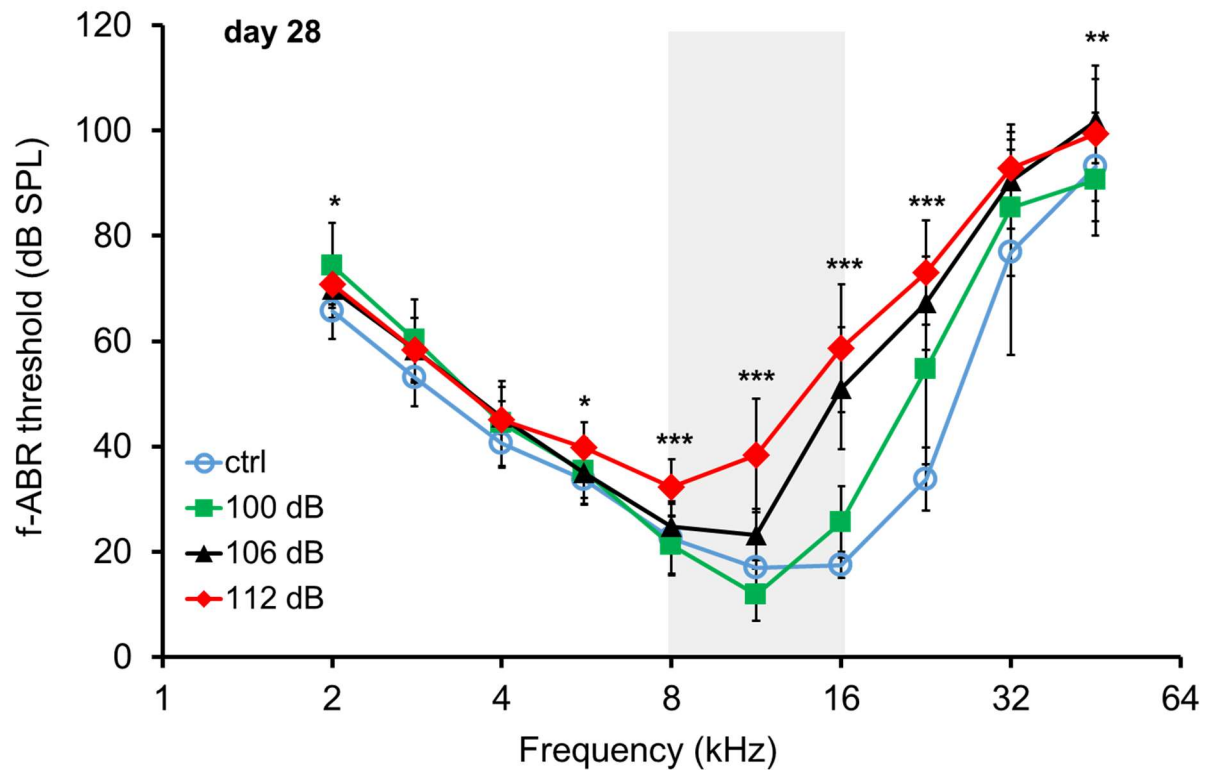
Figure 17. Effects of the strength of noise trauma on frequency-specific ABR thresholds on day 28. Mean threshold shifts ± SD are shown, n = 20 ears for 106 dB SPL, n = 18 ears for 112 dB SPL, n = 16 ears for 100 dB SPL (Nasri, 2023), n = 8 ears for control group. The Kruskal-Wallis/Bonferroni test showed significant differences at 2 kHz (*p* = 0.014), 5.6 kHz (*p* = 0.019), 8 kHz through 22.6 kHz (*p* ≤ 0.001) and 45.2 kHz *(p* = 0.002). Precise pair analysis is given in Table 3.

Table 3. Statistical analysis the effect of trauma strength on f-ABR thresholds on day 28. The *p*-values of a detailed pair analysis of the Kruskal-Wallis/Bonferroni test are listed, cf. Fig. 17, where also n-numbers are listed.

pair f (kHz)	ctrl	100	ctrl	106	ctrl	112	100	106	100	112	106	112
2	0.015		ns		ns		ns		0.004		0.036	
5.6	ns		ns		ns		ns		ns		ns	
8	ns		ns		0.008		ns		<0.001		0.008	
11.3	ns		ns		ns		0.004		ns		ns	
16	ns		<0.001		<0.001		0.001		<0.001		ns	
22.6	ns		0.001		<0.001		ns		0.021		ns	
45.2	ns		ns		ns		0.006		0.023		ns	

5.2.2 Threshold shifts in frequency-ABR

5.2.2.1 Time course of trauma-induced damage

Figure 18 shows frequency-specific threshold shifts on day 28 with regard to day -2. All trauma groups and the control group are displayed together. This shift could also be labelled as "total damage" after 4 weeks and includes an increase in hearing threshold by the respective noise trauma (PTS) and a smaller one induced by aging. The diagram reveals that the extent of damage is linked to the intensity of noise trauma. Most affected frequencies are located within the 5.6 kHz to 22.6 kHz range. At 32 kHz and 45.2 kHz, the differences are not statistically significant. It should be noted there is a large standard deviation of the data, especially at 32 kHz. Another reason might lie in the fact that thresholds of 105 dB SPL were arbitrarily assigned if the range of operation of our device Audiology_Lab was exceeded (Otoconsult, Marcus Müller, Frankfurt/Main, Germany).
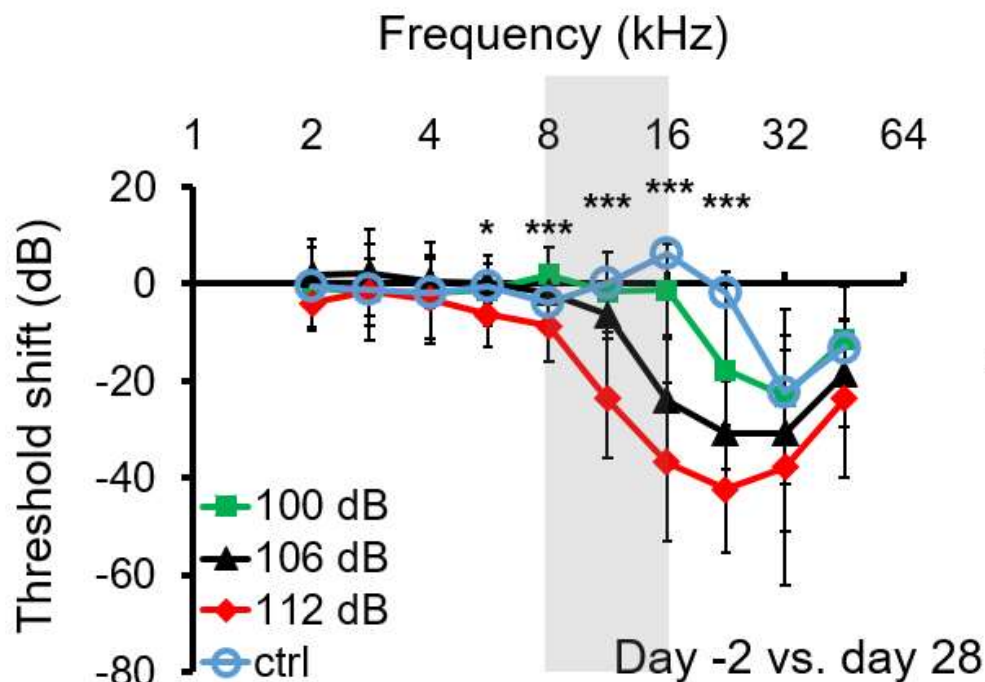
Figure 18. Effects of the strength of noise trauma on frequency-specific threshold shifts four weeks after trauma. The threshold shift represents the difference in hearing thresholds between day -2 and day 28. Mean threshold shifts ± SD are shown (data for the 100 dB SPL trauma group from (Nasri, 2023) – for n = 8 ears (control group), n = 16 ears (100 dB SPL trauma group), n = 20 ears (for both 106 dB SPL and 112 dB SPL, except n = 18 ears on day 28 of the latter). The Kruskal-Wallis/Bonferroni test yielded significant differences at 5.6 kHz ($p = 0.014$), 8 kHz ($p = 0.001$), 11.3 kHz ($p < 0.001$), 16 kHz ($p < 0.001$) and 22.6 kHz ($p < 0.001$). Precise pair analysis is given in Table 4. The light grey bar reflects the trauma octave band.

Table 4. Statistical analysis of the effect of trauma strength on frequency-specific threshold shifts between day -2 and day 28. The *p*-values of a detailed pair analysis of the Kruskal-Wallis/Bonferroni test, cf. Figure 18, where also n-numbers are given.

pair f (kHz)	ctrl	100	ctrl	106	ctrl	112	100	106	100	112	106	112
5.6	ns		ns		ns		ns		ns		0.014	
8	ns		ns		ns		ns		<0.001		0.043	
11.3	ns		ns		<0.001		ns		<0.001		0.002	
16	ns		0.002		<0.001		0.004		<0.001		ns	
22.6	ns		0.008		<0.001		ns		0.002		ns	

So far, the consequences of the traumata were depicted only right after and 28 days after the trauma. Figure 19 A shows frequency-specific f-ABR threshold shifts on day 1 with respect to day -2 for the three trauma groups. The frequency range in which thresholds were most affected were located in the 2 kHz to 11.3 kHz range, contrary to day 14 and day 28.

Figure 19 B shows frequency-specific f-ABR threshold shifts on day 14 with respect to day -2 for the three trauma groups. The diagram reveals similar characteristics as on day 28. F-ABR thresholds were mostly affected at frequencies in the 8 kHz to 22.6 kHz range.
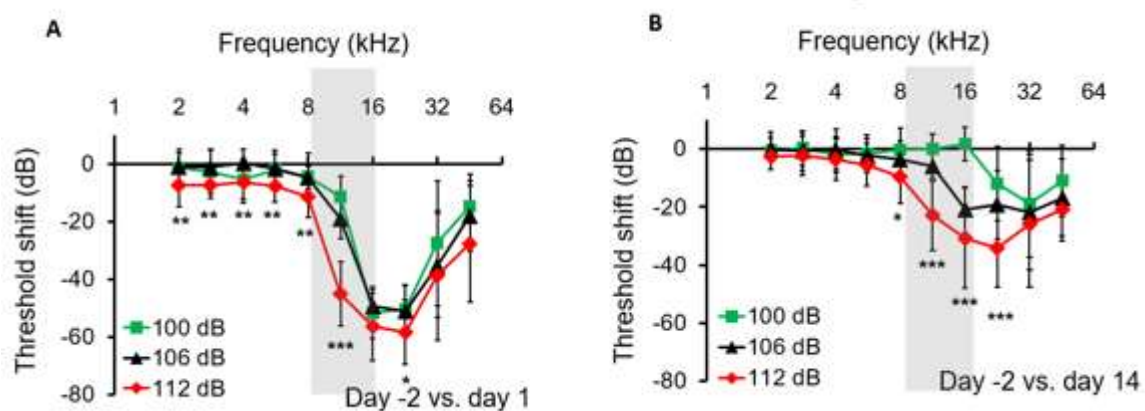
Figure 19. Effects of the strength of noise trauma on frequency-specific threshold shifts one day and 14 days after trauma. Mean threshold shifts ± SD for the three trauma groups between day -2 vs. day 1 (**A**) and day -2 vs. day 14 (**B**). Data for 100 dB SPL from (Nasri, 2023), n = 16 ears for the 100 dB SPL trauma, n = 20 ears for both the 106 dB SPL and the 112 dB SPL trauma, respectively. The Kruskal-Wallis/Bonferroni test yielded significant differences between groups in (**A**) at 2 kHz (*p* = 0.005), 2.8 kHz (*p* = 0.009), 4 kHz (*p* = 0.007), 5.6 kHz (*p* = 0.007) 8 kHz (*p* = 0.005), 11.3 kHz (*p* < 0.001), and 22.6 kHz (*p* = 0.018), respectively for (**B**) at 8 kHz (*p* = 0.015), 11.3 kHz (*p* < 0.001), 16 kHz (*p* < 0.001), and 22.6 kHz (*p* < 0.001). Precise pair analyses are given in Table 5 and 6. The light grey bar reflects the trauma octave band.

Table 5. Statistical analysis of the strength of noise trauma on frequency-specific threshold shifts between day -2 and day 1 after trauma. The *p*-values of a detailed pair analysis of the Kruskal-Wallis/Bonferroni test of the data presented in Figure 19 A.

pair f (kHz)	100	106	100	112	106	112
2	ns		0.023		0.01	
2.8	ns		ns		0.008	
4	0.039		ns		0.011	
5.6	ns		ns		0.008	
8	ns		0.004		0.008	
11.3	ns		<0.001		<0.001	
22.6	ns		0.035		ns	

Table 6. Statistical analysis of the strength of noise trauma on frequency-specific threshold shifts between day -2 and day 14 after trauma. The *p*-values of a detailed pair analysis of a Kruskal-Wallis/Bonferroni test of the data presented in Figure 19 B.

pair f (kHz)	100	106	100	112	106	112
8	ns		0.014		ns	
11.3	ns		<0.001		0.001	
16	<0.001		<0.001		ns	
22.6	ns		<0.001		0.011	

5.2.2.2 Capacity of recovery from noise trauma

To illustrate the effects of noise trauma strength and passage of time on the recovery from trauma, the differences between f-ABR thresholds right after the trauma (day 0) and days 1, 14, and 28, respectively, are depicted in Figure 20. Whereas previous representations of thresholds differences between day -2 (pre-trauma) and day 28 (Fig. 18) reflect the absolute damage, Figure 20 represents the capacity of recovery. On day 28 (Fig. 20 C), a similar recovery capacity for all frequencies is visible except for 4, 16, and 45.2 kHz.
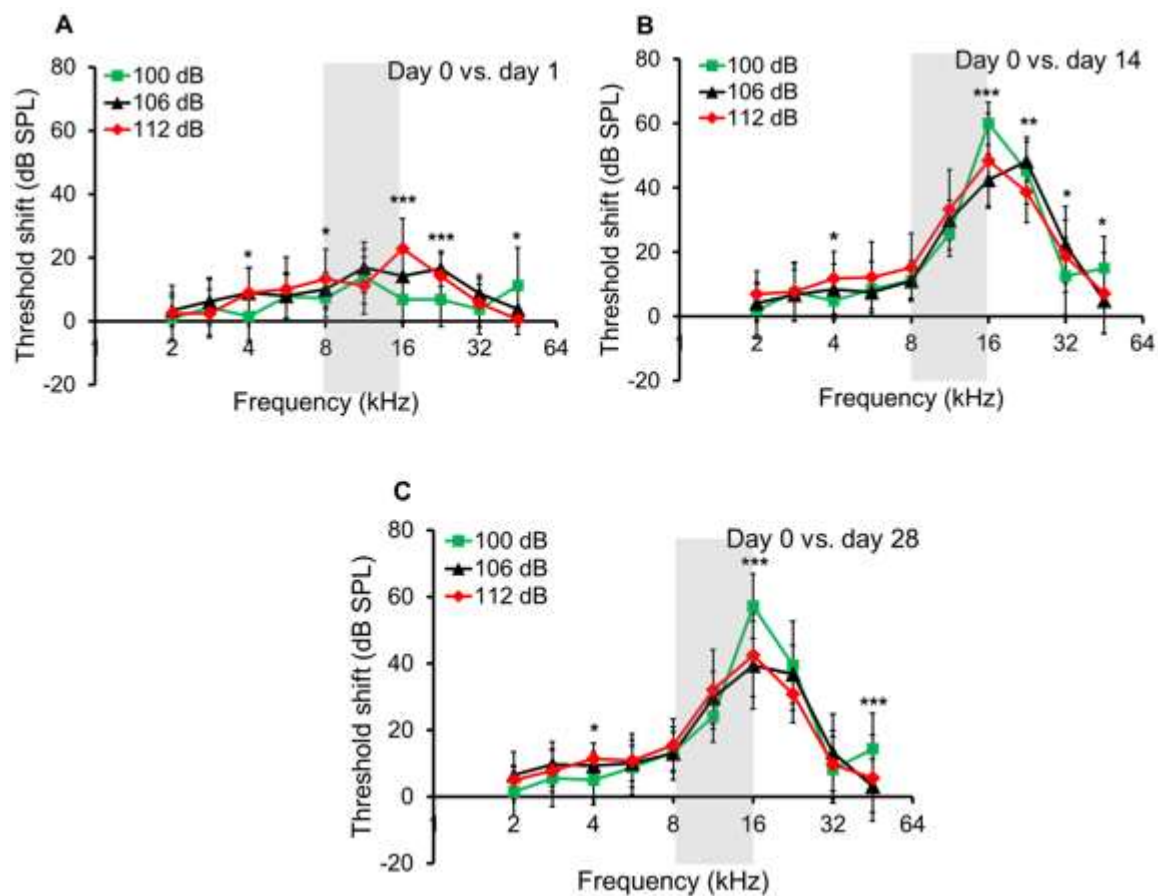
Figure 20. Effects of the strength of noise trauma on the recovery of f-ABR threshold shifts after trauma. Mean threshold shifts ± SD of the three trauma groups are shown with respect to day 0 for day 1 (**A**), day 14 (**B**), and day 28 (**C**) post-trauma. Data for the 100 dB SPL trauma from (Nasri, 2023). N = 16 ears for 100 dB SPL trauma group, n = 20 ears for both the 106 dB SPL and 112 dB SPL trauma. The Kruskal-Wallis/Bonferroni analysis yielded significant differences for (**A**): 4 kHz ($p = 0.019$), 8 kHz ($p = 0.03$), 16 kHz ($p < 0.001$), 22.6 kHz ($p < 0.001$) and 45.2 kHz ($p = 0.04$), (**B**): 4 kHz ($p = 0.037$), 16 kHz ($p < 0.001$), 22.6 kHz ($p = 0,007$), 32 kHz ($p = 0.042$) and 45.2 kHz ($p = 0.019$) and (**C**): significant differences at 4 kHz ($p = 0.015$), 16 kHz ($p < 0.001$) and 45.2 kHz ($p = 0.001$). Detailed pair analyses in Table 7-9. The light grey bar represents the trauma octave band.

Table 7. Effects of trauma strength on recovery of f-ABR thresholds one day after trauma. Detailed pair analysis (*p*-values) of the Kruskal-Wallis/Bonferroni analysis of the data in Figure 20 A.

pair f (kHz)	100	106	100	112	106	112
4	0.042		0.036		ns	
8	ns		0.027		ns	
16	ns		<0.001		ns	
22.6	0.001		0.005		ns	
45.2	ns		0.003		ns	

Table 8. Effects of trauma strength on recovery of f-ABR thresholds 14 days after trauma. Detailed pair analysis (*p*-values) of the Kruskal-Wallis/Bonferroni analysis of the data in Figure 20 B.

pair f (kHz)	100	106	100	112	106	112
4	ns		0.031		ns	
16	<0.001		0.004		ns	
22.6	ns		ns		0.006	
32	0.039		ns		ns	
45.2	0.021		ns		ns	

Table 9. Effects of trauma strength on recovery of f-ABR thresholds 28 days after trauma. Detailed pair analysis (*p*-values) of the Kruskal-Wallis/Bonferroni analysis of the data in Figure 20 C.

pair f (kHz)	100	106	100	112	106	112
4	ns		0.012		ns	
16	0.001		0.001		ns	
45.2	0.002		0.008		ns	

5.3 Effects of noise traumata on ABR peak latencies evoked by click stimulation

According to a number of publications (Gourévitch et al., 2009; Kurt et al., 2009; Mehraei et al., 2016; Rüttiger et al., 2017; Shi et al., 2015; Song et al., 2016; Takazawa et al., 2012), a change in peak latencies can be considered as biomarker for synaptopathy or hidden hearing loss.

In this chapter, peak latencies of responses to click stimulation measured at 40 dB over threshold are evaluated.
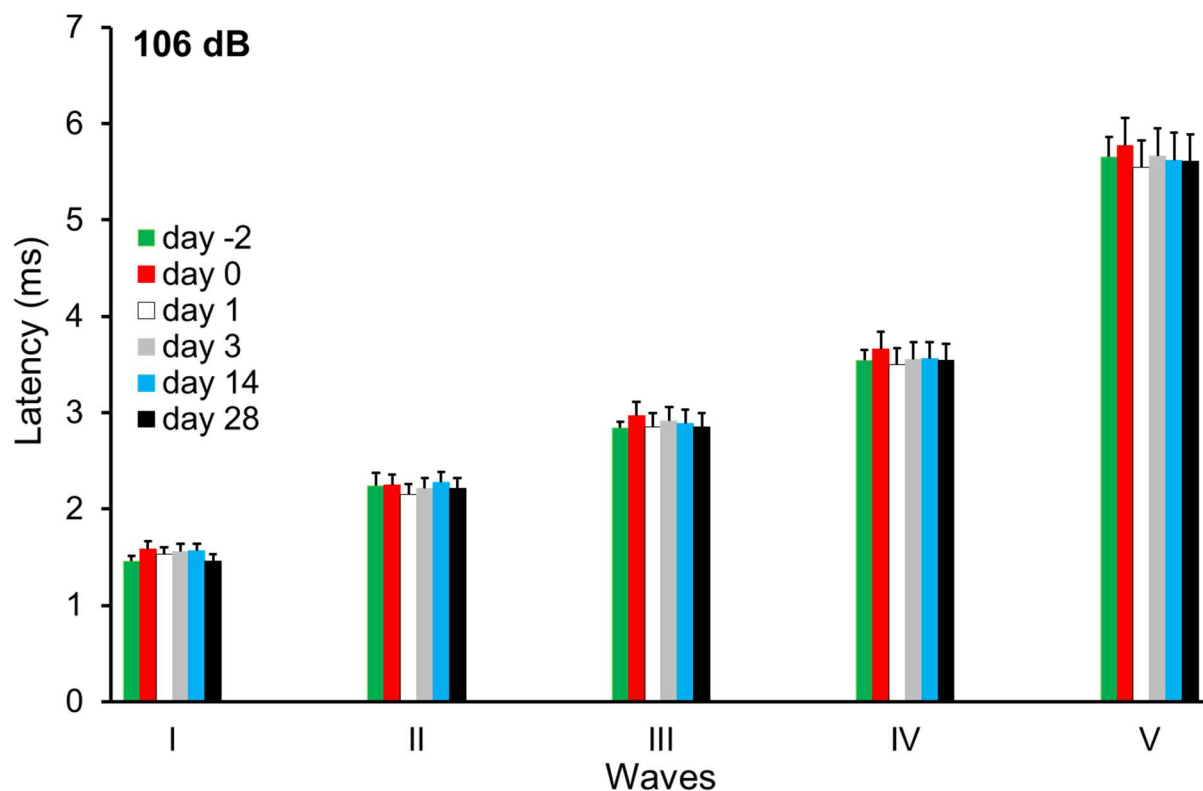
Figure 21. Latencies of responses to click stimulation of the waves I to V were not changed by a 106 dB SPL trauma within a period of four weeks. There were no significant changes in mean peak latency ± SD at 40 dB over threshold between day -2 and day 28 (Wilcoxon signed test) for any of the click-ABR waves I to V. N = 20 ears for each wave.

For each of the click-ABR waves I to V, average peak latencies at 40 dB over threshold were not significantly changed by the 106 dB SPL trauma between day -2 (pre-trauma) and day 28 in any wave (Fig. 21, Wilcoxon signed test). This result was confirmed by the Friedman/Bonferroni test (Table 10). However, this test showed a few significant differences within each wave except wave V, which was due to statistically significant shifts of peak latencies in other pairs, for example day -2 and day 0 in Wave I. Table 10 shows an example of pair analysis of the Friedman/Bonferroni test of Wave I.

Table 10. Detailed pair analysis of the Friedman/Bonferroni test of peak latencies of wave I in the 106 dB SPL trauma group. Red cells indicate an increase of peak latency, the green cell a decrease. All other pair analyses did not yield significant differences. N = 20 ears.

p-value	day-2	day0	day1	day3	day14	day28
day-2	ns	<0.001	ns	<0.001	<0.001	ns
day0	ns	ns	ns	ns	ns	0.013

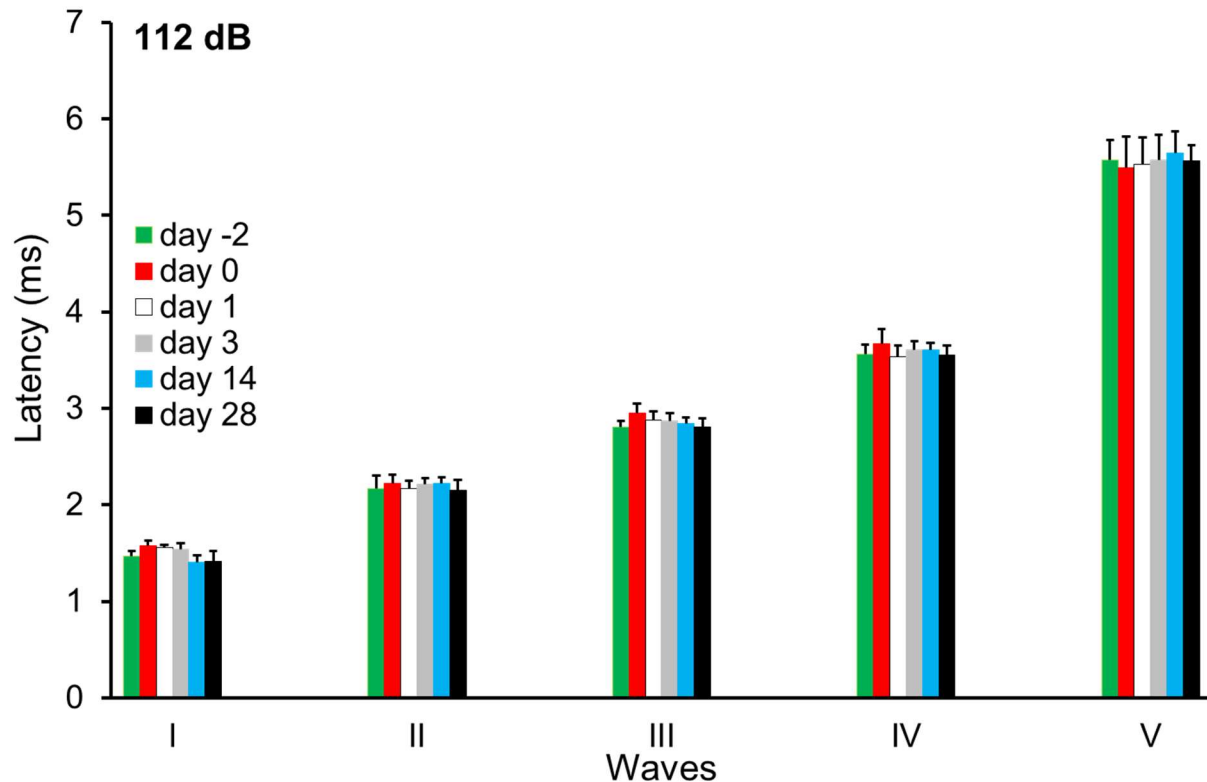**Figure 22. Latencies of responses to click stimulation of the waves I to V were not changed by a 112 dB SPL noise trauma within a period of four weeks.** There were no significant changes in mean peak latency ± SD at 40 dB over threshold for day -2 (pre-trauma) versus day 28 for any of the click-ABR waves I to V (Wilcoxon signed test). N = 20 ears for each wave, except day 0 (n = 15 ears) and day 28 (n = 18 ears).

Similar to the results of the 106 dB SPL trauma, mean peak latencies of the 112 dB SPL trauma group at 40 dB over threshold did not show any significant difference of peak latencies between day -2 (pre-trauma) and day 28 in any wave (Fig. 22, Wilcoxon signed test). This was confirmed in the Friedman/Bonferroni test, which nonetheless showed significant differences between several days of measurement for waves I, III and IV. Just as in the 106 dB SPL trauma group, this was due to statistically significant shifts of peak latencies in pairs different from day -2 versus day 28, i.e. between day 0 and day 14 in wave I.

Table 16 (annex) shows the very few significant differences in latency of day -2 (pre-trauma) versus any other posttraumatic day in waves I-V in the two trauma groups.
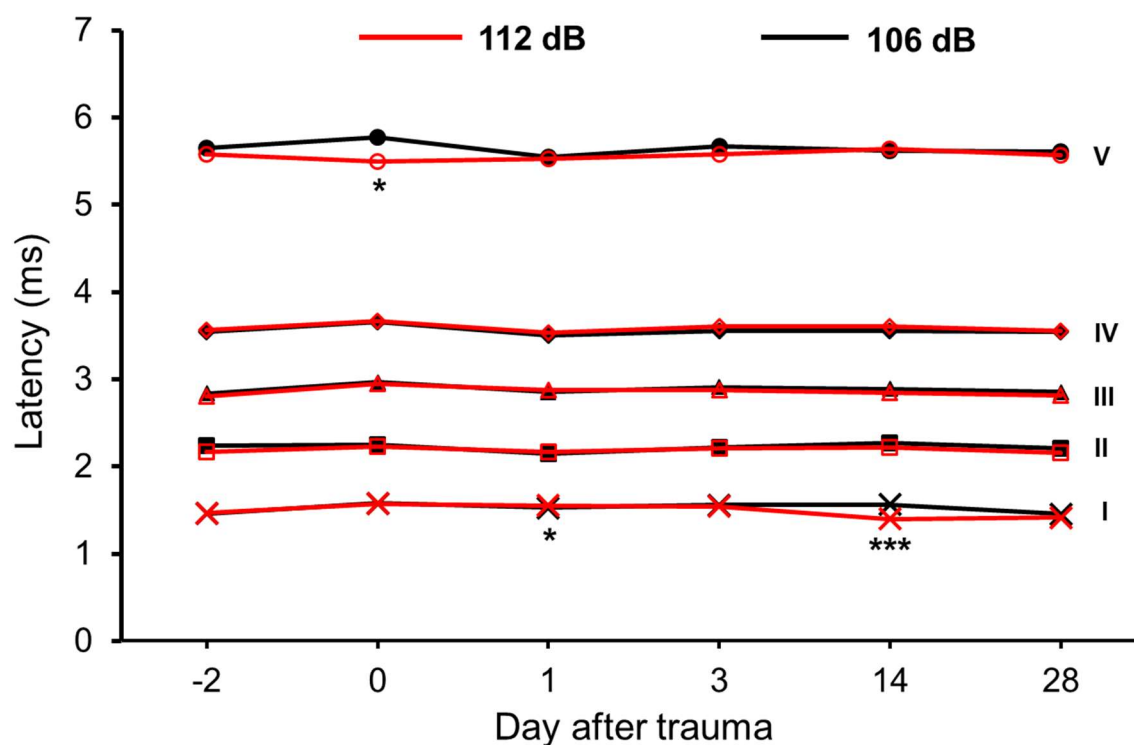
Figure 23. Comparison of the changes in mean peak latencies evoked by click-stimulation after a 106 dB SPL and a 112 dB SPL noise trauma for the ABR waves I to V. Latencies were determined from responses to clicks at 40 dB SPL over threshold. N = 20 ears, except for day 0 (n = 15 ears) and day 28 (n = 18 ears) in the 112 dB SPL trauma group. Significant differences were tested for a given day and a given wave (Mann-Whitney-U-test) and are marked with asterisks: Day 0 for wave V (p = 0.05), day 1 for wave I (p = 0.05), day 14 for wave I ($p < 0.0001$).

Figure 23 shows the direct comparison of time-dependent latencies of click-ABR responses of two trauma groups (106 versus 112 dB SPL) at 40 dB over threshold for each of the ABR waves I to V. There were very few statistical differences between the consequences of the traumata but not on the last day of the experiment, day 28.

Taking the three diagrams from this chapter 5.3 into consideration, the two noise traumata (106 dB SPL, 112 dB SPL) had no effect on mean click latencies.

5.4   Effects of noise traumata on wave I-V amplitudes evoked by click-ABR

A reduction in amplitude of ABR waves, especially wave I, is considered an important bio-marker for synaptopathy, noise-induced hidden hearing loss (NIHHL) and noise-induced hear-ing loss (NIHL), as explained in Chapter 3.3. It can be evaluated by both stimulation of clicks and pure tones. All diagrams of Chapter 5.4 show click amplitudes measured in response to stimulation 40 dB above threshold. Figure 24 shows the change of click amplitudes of waves I to V throughout the course of the experiments for the 106 dB SPL trauma group. There was a significant reduction in mean amplitudes between day -2 (pre-trauma) versus day 28 in all waves (Wilcoxon signed test). However, amplitude reductions were largest for wave I (-38.6%) and wave III (-32.9%), whereas wave II (-27.6%), wave IV (-15.1%) and wave V (-17.6%) were more stable.
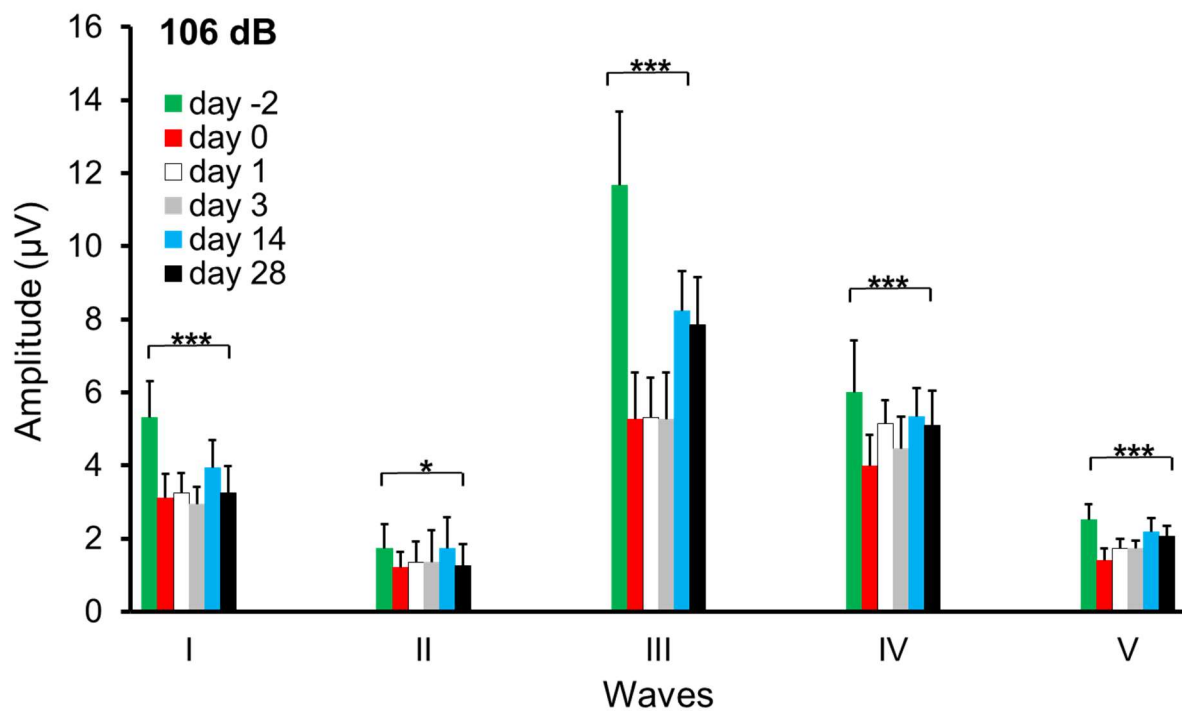
Figure 24. The amplitudes of click ABR waves I - V were reduced by the 106 dB SPL noise trauma four weeks after trauma. The average amplitude was determined at 40 dB over threshold, n = 20 ears. Significant reductions (Wilcoxon signed test between day -2 and 28) were found for wave I ($p < 0.001$), wave II ($p = 0.014$), wave III ($p < 0.001$), wave IV ($p = 0.001$) and wave V ($p < 0.001$).

For the 112 dB SPL trauma group, the reduction of click amplitudes of waves I to V is shown in Figure 25. Waves I and III showed the strongest decrease on day 28 compared to day -2 (-46.9% and -46.3% respectively). The mean amplitude of wave II was unchanged on day 28 versus day -2, but amplitudes of waves IV and V were also reduced on day -28 (-22.5 and -15.4% respectively).

Taken together, the click amplitudes of almost all ABR waves, especially those of waves I and III, were strongly reduced by a trauma of 106 dB SPL after 4 weeks, and even stronger after a trauma of 112 dB SPL.
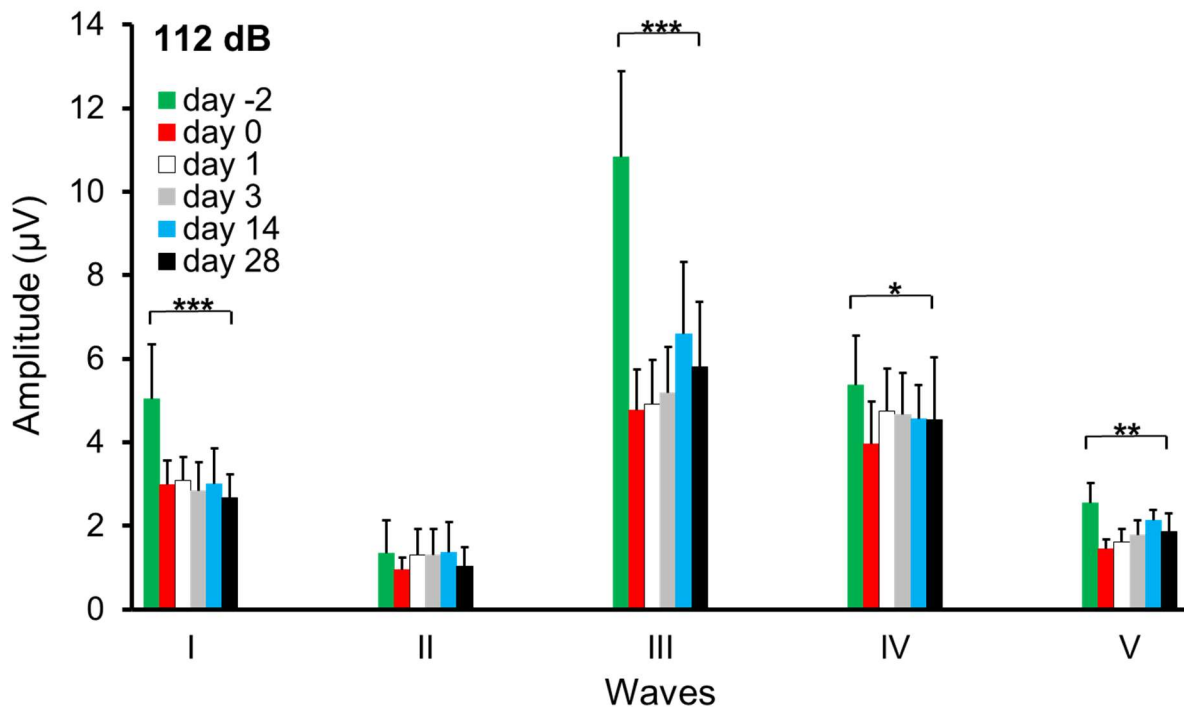
Figure 25. The amplitudes of click ABR waves I, III, IV, and V were reduced by the 112 dB SPL noise trauma four weeks after trauma. The average amplitude was determined at 40 dB over threshold, n = 20 ears, except day 0 (n = 15 ears) and day 28 (n = 18 ears). Significant reductions (Wilcoxon signed test between day -2 and day 28) were observed for wave I ($p < 0.001$), wave III ($p < 0.001$), wave IV ($p = 0.011$) and wave V ($p = 0.002$).

5.5 Effects of noise traumata on growth functions of the amplitude of wave I

5.5.1 Effects of noise traumata on growth functions evoked by click stimulation

The amplitude of wave I depends on the kind of stimulation (click stimulation versus frequency-specific stimulation) and on the level of stimulation. The higher the stimulus level, the higher the amplitude of wave I, because more and more fibers of the auditory nerve (ANF) are recruited (Ia, Ib, Ic). A graph that displays wave I amplitude as a function of stimulus level is called growth function of wave I. Figure 26 shows mean growth functions of wave I from click ABR data for the pre-trauma day (day -2), as well as day 14 and day 28 after the 106 dB SPL trauma.

It should be noted that amplitude data were taken with regard to the respective threshold, starting at 10 dB SPL over threshold (Figure 26). For all levels from 10 to 50 dB over threshold, amplitudes were significantly reduced 28 days after trauma, with the most significant reduction of amplitude of wave I (-38.7%) on day 28 vs. pre-trauma at 40 dB over threshold. These results indicate that part of the functional synaptic connections were destroyed 4 weeks after the 106 dB SPL trauma such that fewer ANFs contributed to the wave I amplitude signal.
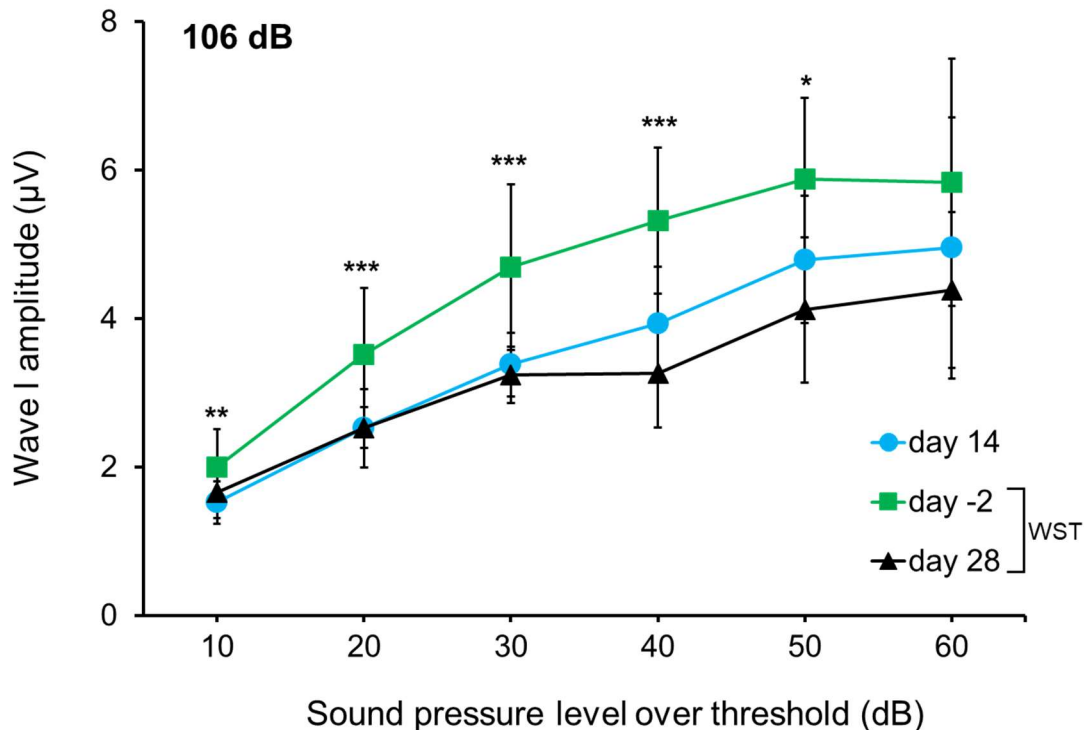
Figure 26. Effects of the 106 dB SPL trauma on growth functions of the amplitude of wave I evoked by click stimulation. Average amplitudes of wave I ± SD are shown as function of sound pressure level over threshold ('growth function') for experimental days -2 (pre-trauma), 14, and 28. N = 20 ears, except for 60 dB SPL over threshold: n = 14 ears on day -2, n = 6 ears on day 14 and 28; Wilcoxon signed test (WST). The *p*-values are shown in Table 11.

Table 11. Statistical analysis (Wilcoxon signed test) of the level-dependent wave I amplitudes before and 28 days after the 106 dB SPL trauma (cf. Fig. 26).

	10 dB	**20 dB**	**30 dB**	**40 dB**	**50 dB**
_p_-value	0.006	≤0.001	≤0.001	≤0.001	0.05

Next, the consequences of the 112 dB SPL trauma on amplitudes of wave I were evaluated. Growth functions for wave I display a similar picture as in the 106 dB SPL trauma, with an even larger reduction (-46.8%) of the amplitude of wave I at 40 dB over threshold 28 days after the trauma (Fig. 27).
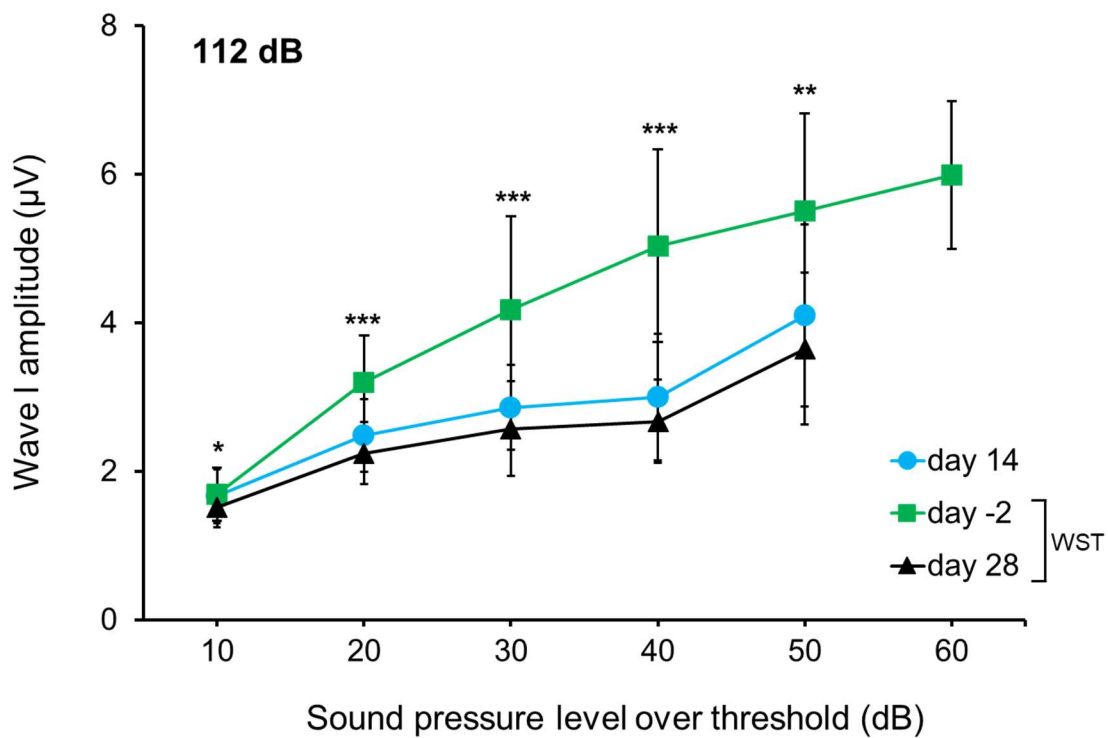
Figure 27. Effects of the 112 dB SPL trauma on growth functions of the amplitude of wave I evoked by click stimulation. Average amplitudes of wave I ± SD are shown as function of sound pressure level over threshold ('growth function') for experimental days -2 (pre-trauma), 14, and 28. At 50 dB SPL over threshold: n = 19 ears on day 14, n = 16 ears on day 28. N = 18 ears for the rest of day 28 data. N = 20 ears for all remaining data; Wilcoxon signed test (WST). The _p_-values are shown in Table 12.

Table 12. Statistical analysis (Wilcoxon signed test) of the level-dependent wave I amplitudes before and 28 days after the 112 dB SPL trauma (cf. Fig. 27).

	10 dB	**20 dB**	**30 dB**	**40 dB**	**50 dB**
_p_-value	0.022	≤0.001	0.001	≤0.001	0.002

5.5.2 Effects of noise traumata on wave I growth functions evoked by frequency-ABR

This chapter is dedicated to growth functions of wave I evoked by frequency-specific stimulation of the 106 dB SPL trauma group. Figures 24 and 26 show severe decreases of amplitudes of wave I in response to click stimuli on day 28 compared to day -2. Here, this phenomenon was examined through the frequency perspective. The 106 dB SPL trauma caused a permanent frequency-dependent absolute threshold shift 4 weeks after trauma, starting at 11.3 kHz and continuing up to 45.2 kHz (the highest frequency measured). For these hardest-hit frequencies, mean ABR wave I amplitudes from day -2 and day 28 are presented as functions of the (absolute) sound pressure level (Figures 28-31). This leads to a shift of the growth function on day 28 along the x-axis, which represents the increase in hearing threshold (cf. Figs. 14, 17, 18).
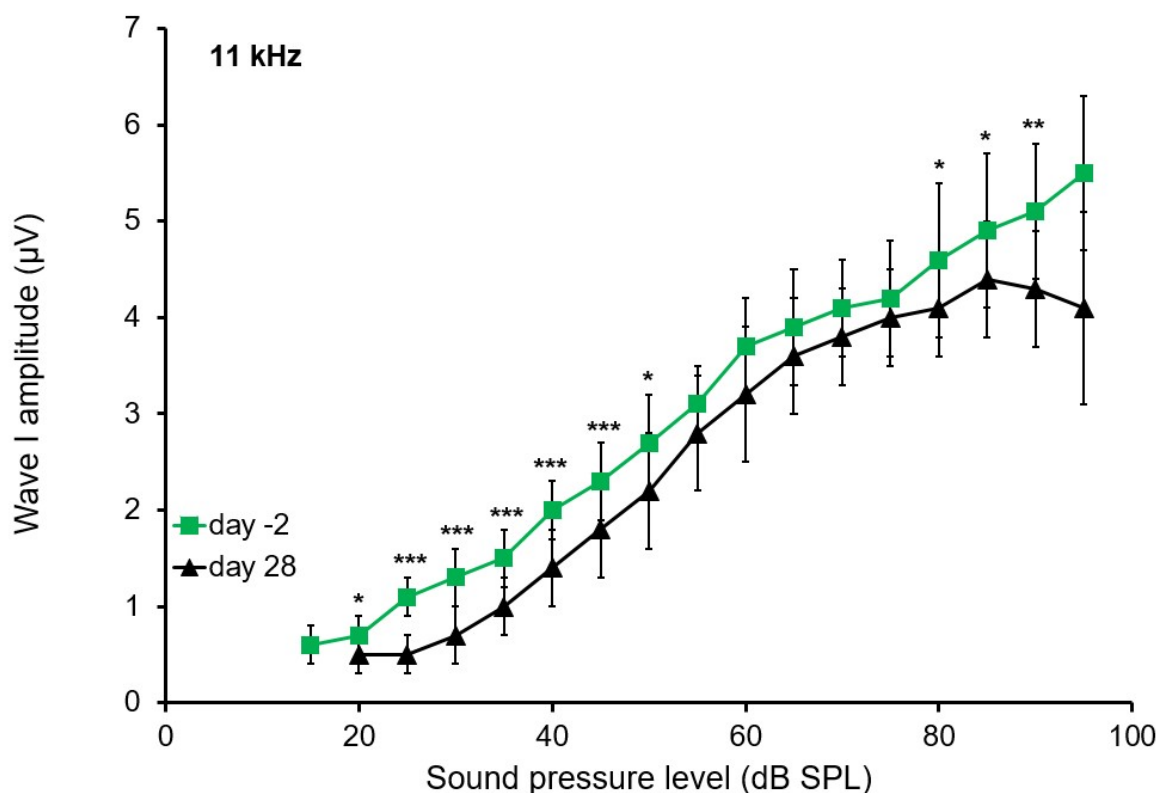
Figure 28. Effects of the 106 dB SPL trauma on the growth function of the amplitude of wave I at 11 kHz. Average amplitudes ± SD for day -2 (pre-trauma) and 28 days after trauma; Wilcoxon signed test, day -2: n = 20 ears for all dB SPL, except 15 dB SPL (n = 11 ears), 20 dB SPL (n = 18 ears) and 95 dB SPL (n = 5 ears); on day 28 n = 20 ears, except 20 dB SPL (n = 10 ears), 25 dB SPL (n = 15 ears), 90 dB SPL (n = 18 ears) and 95 dB SPL (n = 4 ears). The *p*-values for pair analysis in Table 13.

For 11 kHz, the shift in threshold was mild (5 dB, Fig. 28) whereas it increased to 25 dB at both 16 kHz (Fig. 29) and 22 kHz (Fig. 30) and to as much as 55 dB at 32 kHz (Fig. 31). Besides a small threshold shift, the 106 dB SPL trauma led to a significant reduction of the amplitudes of wave I at 11 kHz for many sound pressure levels (20 - 50 and 80 – 95 dB SPL) indicating that functional connections between IHC active zones and ANF type I were destroyed. Table 13

displays the corresponding statistical analysis whereas Table 14 shows the mean reduction of wave I amplitudes expressed as a percentage 28 days after trauma versus pre-trauma.

For the 16 kHz stimulation frequency (Fig. 29), the 106 dB SPL trauma caused a significant reduction in amplitude at all decibel steps from 50 to 95 dB SPL, in line with the threshold shift (Fig. 14) and decreases of click amplitudes (Fig. 24 and 26). The strongest decline was observed at 65 dB SPL with a 69.2% drop in amplitude. Table 13 shows the statistical analysis of the amplitudes of wave I at 16 kHz between day -2 and day 28 after trauma whereas Table 14 illustrates the drop in mean amplitudes with respect to pre-trauma.

Figure 29. Effects of the 106 dB SPL trauma on the growth function of the amplitude of wave I at 16 kHz. Average amplitudes ± SD for day -2 (pre-trauma) and 28 days after trauma; Wilcoxon signed test, on day -2 n = 20 ears for all dB SPL, except 20 dB SPL (n = 4 ears), 25 dB SPL (n = 9 ears), 30 dB SPL (n = 17 ears), 95 dB SPL (n = 12 ears) and 100 dB SPL (n = 3 ears); on day 28 n = 20 ears, except 45 dB SPL (n = 6 ears), 50 dB SPL (n = 10 ears), 55 dB SPL (n = 17 ears), 60 dB SPL (n = 18 ears), 65/70 dB SPL (n = 19 ears), 90 dB SPL (n = 10 ears) and 95 dB SPL (n = 18 ears). *P*-values for pair analysis in Table 13.

Figure 30 shows the growth functions of the amplitude of wave I for a 22 kHz tone pip stimulation. Besides a threshold shift of 25 dB, a significant reduction of the amplitudes from 65 to 100 dB SPL is visible 4 weeks after trauma. The largest reduction (72.2 %) was found at 80 dB SPL. Table 13 gives the details of the statistical analysis of the amplitudes at 22 kHz

whereas Table 14 summarizes the mean reduction of the amplitude values four weeks after the trauma.
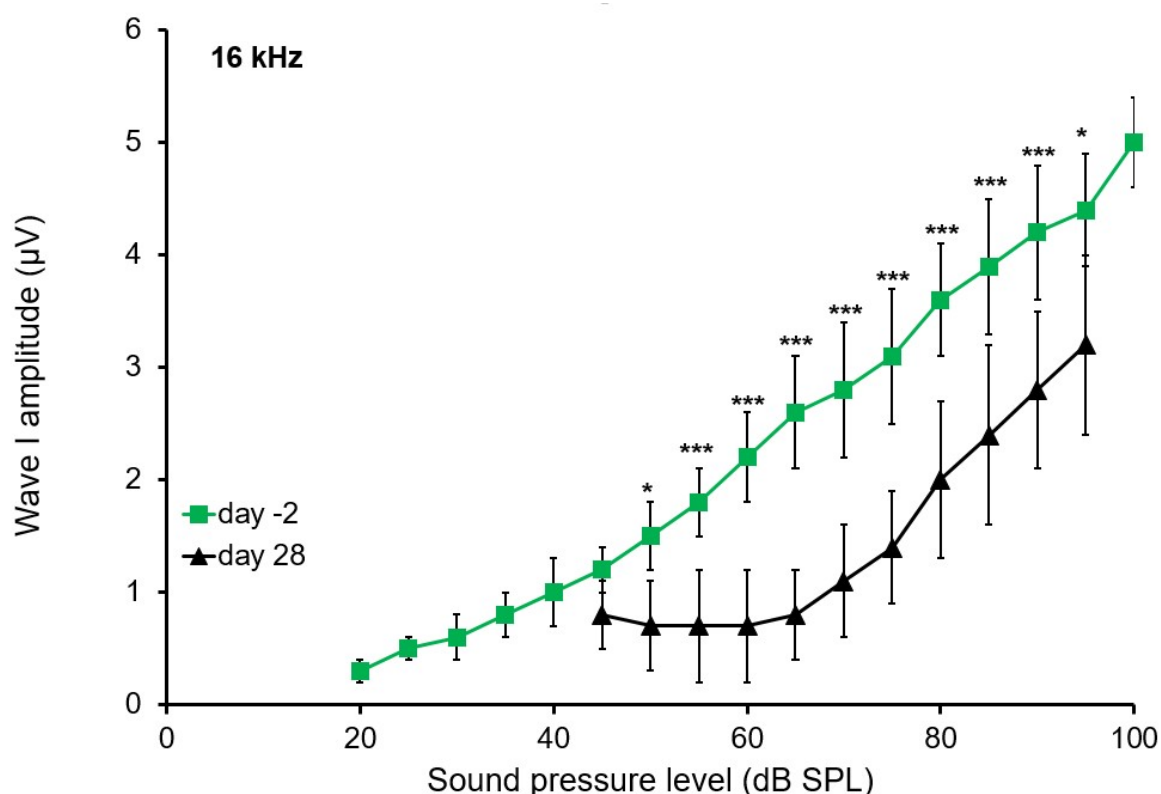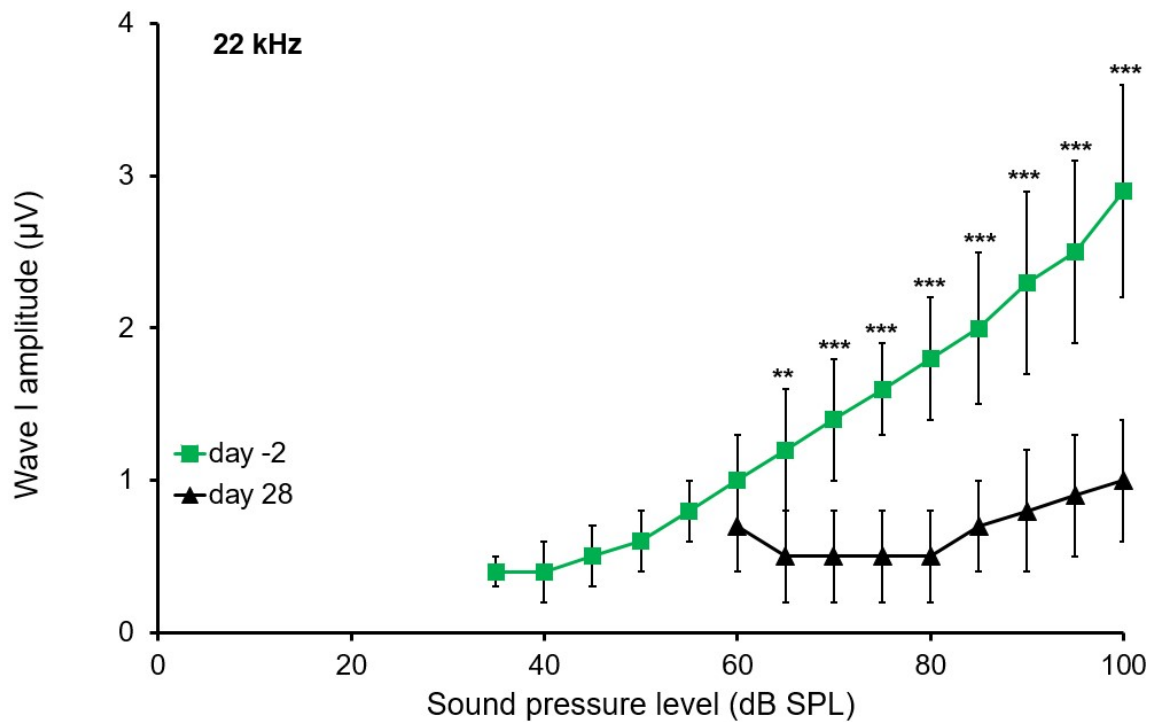

Figure 30. Effects of the 106 dB SPL trauma on the growth function of the amplitude of wave I at 22 kHz. Average amplitudes ± SD for day -2 (pre-trauma) and 28 days after trauma; Wilcoxon signed test, on day -2 n = 20 ears for all dB SPL, except 35 dB SPL (n = 14 ears), 40 dB SPL (n = 17 ears), 45 dB SPL (n = 19 ears), 50 dB SPL (n = 19 ears) and 55 dB SPL (n = 19 ears), on day 28 n = 20 ears, except 60 dB SPL (n = 4 ears), 65 dB SPL (n = 11 ears), 70 dB SPL (n = 15 ears) and 75 dB SPL (n = 18 ears), 80 dB SPL (n = 18 ears) and 85 dB SPL (n = 19 ears). The *p*-values for pair analysis in Table 13.

Table 13. Statistical analysis (Wilcoxon signed test) of the level-dependent wave I amplitudes at 11, 16, and 22 kHz before and 28 days after the 106 dB SPL trauma (cf. Fig. 28-30).

11 kHz	20 dB	25 dB	30 dB	35 dB	40 dB	45 dB	50 dB	80 dB	85 dB	90 dB
p-value	0.015	0.001	<0.001	<0.001	<0.001	0.001	0.035	0.038	0.015	0.009

16 kHz	50 dB	55 dB	60 dB	65 dB	70 dB	75 dB	80 dB	85 dB	90 dB	95 dB
p-value	0.028	0.001	<0.001	<0.001	<0.001	0.001	0.035	<0.001	0.001	0.036

22 kHz	65 dB	70 dB	75 dB	80 dB	85 dB	90 dB	95 dB	100 dB
p-value	0.004	0.001	<0.001	<0.001	<0.001	<0.001	<0.001	<0.001

Table 14. Reduction of mean amplitudes of Wave I on day 28 compared with day -2 for 11, 16, and 22 kHz (cf. Fig. 28-30). Only data pairs with statistically significant differences are listed.

11 kHz	20 dB	25 dB	30 dB	35 dB	40 dB	45 dB	50 dB	80 dB	85 dB	90 dB
Ampli-tude	-28.6%	-54.5%	-46.2%	-33.3%	-30%	-21.7%	-18.5%	-10.9%	-10.2%	-15.7%

16 kHz	50 dB	55 dB	60 dB	65 dB	70 dB	75 dB	80 dB	85 dB	90 dB	95 dB
Ampli-tude	-53.3%	-61.1%	-68.2%	-69.2%	-60.7%	-54.8%	-44.4%	-38.5%	-33.3%	-27.3%

22 kHz	65 dB	70 dB	75 dB	80 dB	85 dB	90 dB	95 dB	100 dB
Ampli-tude	-58.3%	-64.5%	-68.8%	-72.2%	-65%	-65.2%	-64%	-65.5%

Figure 31. Effects of the 106 dB SPL trauma on the growth function of the amplitude of wave I at 32 kHz. Average amplitudes ± SD for day -2 (pre-trauma) and 28 days after trauma. Number of ears measured in Table 15. There are no statistically significant differences.

Figure 31 shows mean ABR wave I amplitude responses on day -2 and 28 days after the 106 dB SPL trauma in response to 32 kHz tone pips. The trauma caused a huge threshold shift by 55 dB. Only for the levels 90, 95, and 100 dB SPL, ABR wave I could be determined for a minimum of 3 ears. Mean values on day 28 appear to be smaller than those measured on day -2 for the same level. Due to the large SD and the small number of data between 90 and 100 dB SPL for day 28 there were no statistically significant differences of the amplitudes between day -2 and day 28. This is most likely due to a too small number of ears measured (Table 15) because for the majority of ears the hearing threshold had risen above measurable levels of audiology-lab®.

Table 15. **Number of ears (n) measured in the 106 dB SPL trauma group at 32 kHz.**

n	35 dB	40 dB	45 dB	50 dB	55 dB	60 dB	65 dB	70 dB	75 dB	80 dB	85 dB	90 dB	95 dB	100 dB
day-2	2	5	5	5	8	9	13	14	16	18	18	19	13	13
day28	-	-	-	-	-	-	-	-	-	-	-	9	3	4

Taken together, the 106 dB SPL trauma had not only caused increasing threshold shifts in the range from 11 kHz to 32 kHz but also severe reductions of the level-dependent amplitudes of wave I. Both the range and the degree of amplitude reduction were aggravated with increasing frequencies (11 kHz – 22 kHz). At the highest frequency at which amplitude data could be determined (32 kHz) their number was too small and SD was too large for meaningful statistics. Nevertheless, the frequency-dependent growth functions of amplitude wave I indicate that destruction of functional connections between IHC ribbon synapses and auditory nerve fibers increased with frequency.

6 Discussion

In this thesis, I have studied the effects of two noise traumata, 106 dB SPL and 112 dB SPL from 8 – 16 kHz for two hours, on hearing thresholds and characteristics of ABR waves of C57BL/6N mice. These parameters were analyzed in both click-ABR and f-ABR data over a time span between day 0 – shortly after the trauma – and day 28 and were compared with the pre-trauma situation (day -2). For both the 106 dB SPL and the 112 dB SPL trauma, click thresholds revealed a TTS and a PTS four weeks later. f-ABR thresholds showed that the amount of both TTS and PTS and the frequency range affected scaled with trauma strength. Click-induced amplitudes of ABR wave I were significantly reduced 28 days after both traumata. Similarly, f-ABR revealed reduced growth functions of wave I amplitudes in the mid-to-high frequency range four weeks after the 106 dB SPL trauma. In contrast, peak wave I latencies of click responses were unaltered.

The discussion will focus on the following topics:

- Thresholds and amplitudes of ABR wave I

- Latencies of ABR wave I

- Anesthesia versus wakefulness and the outcome of noise trauma

- Genetics and noise trauma

- Outlook

6.1 Thresholds and amplitudes of ABR wave I

Previous experiments from our lab with a 100 dB SPL noise trauma created a PTS at 45 kHz only (Blum et al., 2024; Nasri, 2023). Regarding the hearing parameters, we therefore nearly reproduced the findings of the landmark publication from 2009 (without any PTS) using CBA/CaJ mice (Kujawa and Liberman, 2009). The traumata used in the present study did not only cause a TTS but also a PTS. Four weeks after the 106 dB SPL trauma, the PTS affected the 11 kHz – 45 kHz range (Fig. 14) whereas the 112 dB SPL trauma caused a PTS in 7 out of 10 frequencies (Fig. 15). Likewise, click-ABR thresholds were increased four weeks after both traumata (Fig. 13). Trauma strengths corresponded to the degree of both TTS and PTS. The range of affected frequencies were monotonic functions of trauma strengths. Wang and Liberman observed similar findings in CBA/CaJ mice, which were exposed to the same noise traumata with either 100, 106, 112, or 116 dB SPL (Wang and Liberman, 2002).

Until recently, OHCs were regarded as the most sensitive structures in the cochlea (Kujawa and Liberman, 2009; Natarajan et al., 2023; Wang and Liberman, 2002). In our study, there

was no significant cellular loss of OHCs in all cochlear regions 4 weeks after the trauma compared with control (Blum et al., 2024). However, a functional deterioration of OHCs leading to reduced electromotility is likely (Rüttiger et al., 2017). This functional OHC damage is expected to be shifted by half an octave above the noise frequency band for the lower trauma; it may further extend to the entire frequency region for the higher trauma because of cochlear non-linearities (Cody and Johnstone, 1981). A reduced cochlear amplifier in turn would have increased the thresholds for IHC activation in a frequency-dependent manner and would have affected both ABR growth functions and ABR thresholds. As we did not record DPOAEs in our experiments we cannot judge the frequency-dependent functional damage of the OHCs. In the original study on NIHHL, Kujawa and Liberman (2009) reported full recovery of both DPOAE amplitudes and ABR thresholds in CBA/CAJ mice 8 weeks after a 100 dB SPL trauma, which led them coin the term "hidden hearing loss". What was hidden was the reduction in ABR wave I amplitudes and in ribbon synapse numbers in the high frequency region (Kujawa and Liberman, 2009).

Besides hearing thresholds, also the amplitudes of wave I will be affected by reduced OHC function. This applies not only to growth functions of ABR wave I at 11, 16, and 22 kHz (Fig. 28 - 30) but also to growth functions of click-ABR amplitudes (Figs. 26, 27) and click-ABR amplitudes (Figs. 24, 25). With regard to click-evoked ABR wave I growth functions, the amplitudes were plotted as a function of level starting at 10 dB above the respective threshold (Figs. 26, 27) such that a threshold shift by OHC malfunction four weeks after trauma is included to some extent. By contrast, growth functions of f-ABR wave I amplitudes plotted as functions of (absolute) sound pressure level (Figs. 28 – 30) indicate both a trauma-dependent shift of thresholds and the decline of the wave I amplitudes. One might argue that the changes in both parameters were caused solely by reduced OHC function. This may largely apply to the threshold shift. However, the loss of up to 50 % of the ribbons four weeks after both traumata (Blum et al., 2024; Schätzle, unpublished) is clearly independent of a potentially reduced OHC function and may explain the reduction of ABR wave I amplitudes to a great extent.

6.2   Latencies of ABR wave I

An increase in latency after noise trauma or sensori-neural impairment has been described in a number of studies (Gourévitch et al., 2009; Kurt et al., 2009; Rüttiger et al., 2017; Shi et al., 2015; Song et al., 2016; Takazawa et al., 2012). Latencies of ABR waves depend on the number of synchronously firing type I nerve fibers. Because of their high spontaneous rate, type Ia fibers clearly dominate wave I (Bourien et al., 2014). Evaluation of the effects of trauma on f-ABR wave I latency function revealed an increase of latency with trauma strength for a given frequency suggesting that not only type Ib and Ic were affected by the traumata but also part

of the threshold-determining fibers type Ia (Blum et al., 2024). In light of this finding, it is surprising that latencies of click-evoked waves I four weeks after trauma did not change versus pre-trauma values for both the 106 dB SPL trauma (Fig. 21, Table 10), and 112 dB SPL trauma (Fig. 22). What needs to be taken into account here is that latency was determined at a level 40 dB over threshold i.e. the click represented was much louder than in the pre-trauma control; and that in click stimulation, higher frequencies are generally under-represented due to technical issues. The higher frequency range, however, is the range most affected by a noise trauma. To summarize, the metric "latency of wave I to click stimulation at 40 dB over threshold" is not a sensitive measure for characterizing noise-induced hearing loss and cochlear synaptopathy.

6.3   Anesthesia versus wakefulness and the outcome of noise trauma

For successful ABR recordings, anesthesia is required because otherwise, movement artifacts will dominate the small extracranial potentials. It is surprising however to see numerous experiments using acoustic overexposure with 100 dB SPL and above being conducted without anesthetics (Gourévitch et al., 2009; Kujawa and Liberman, 2009, 2006; Mehraei et al., 2016; Milon et al., 2018; Shi et al., 2015; Song et al., 2016; Suthakar and Liberman, 2021).

In order to protect the mice from physical suffering during our research, all mice were anesthetized during the noise trauma, which may have caused different effects than in the case of awake mice during noise exposure. Without anesthetics, the stapedius reflex is not diminished and thus physiological noise protection is functional (Gnadeberg et al., 1994; Ohlemiller, 2019).

Various publications reported that the stapedius reflex attenuates sound pressure levels. In one study the effect was estimated at 15 dB SPL, another study revealed that it was strongest at low frequencies, and attenuation could reach a peak of 30 dB SPL (Brask, 1978; Snow et al., 2009). It should be noted that the stapedius reflex is rather short-lived (Habener and Snyder, 1974; Rosenhall et al., 1979) and therefore will not be active during a noise trauma lasting for 2 h.

Another aspect of non-anesthetized mice exposed to noise for 2 h is the massive release of stress hormones such as 11-dehydrocorticosterone (the mouse analogue of cortisone) and the activation of the stress pathway (Vettorazzi et al., 2022). Corticosterone acts in multiple ways but foremost is a transcriptional modulator (Vettorazzi et al., 2022). Recently, a comprehensive study on cell-specific transcriptional changes elicited by a noise trauma (in awake mice) revealed a large number and complexity of changes in gene expression (Milon et al., 2021). It has been shown that mice that were subjected to mild restrained stress, which was accompanied by elevated levels of corticosterone, and to a noise trauma 2 h later, were protected from PTS (Wang and Liberman, 2002).

Mice exposed to noise in an experimental setting where they cannot flee respond with a freezing behaviour (personal communication to J. Engel by Klaus-Peter Richter, IL, USA). In two studies, the effects of noise traumata on anesthetized versus non-anesthetized mice were examined (Jongkamonwiwat et al., 2020; Reijntjes et al., 2020). Reintjes et al. using C57BL/6J and FVB mice revealed a difference neither in PTS/TTS in f-ABR measurements, nor in the number of ribbons/IHC in all cochlear regions (Reijntjes et al., 2020). Jongkamonwiwat et al. exposing FVB mice to 94, 100 and 105 dB SPL traumata observed a greater TTS one to two weeks after trauma in anesthetized versus awake mice. However, PTS thresholds ended up the same for both groups (Jongkamonwiwat et al., 2020). Ketamine-based anaesthesia were used in both studies. In our study, we used fentanyl-based anaesthesia, which is fully antagonizable. Thus duration of anaesthesia could be shortened in frequent ABR measurements (Blum et al., 2024).

6.4   Genetics affect the outcome of noise trauma

A number of recent findings confirmed that different mouse strains do not respond in the same way to noise exposure (Boussaty et al., 2020; Early et al., 2022; Lavinsky et al., 2021; Milon et al., 2021). A recent study compared hearing thresholds and amplitudes of wave I before and after a 2 h noise trauma of 108 dB SPL. However, neither CBA/CaJ nor C57BL/6N were included. The genetically related C57BLKS/J mice showed a rather resistant wave I amplitude after a noise trauma from 2 to 10 kHz at 108 dB SPL (Lavinsky et al., 2021).

In humans, there appears to exist a small number of noise induced hearing loss (NIHL) susceptibility genes. Early et al. revealed through twin studies that approximatively 36 % of variability in susceptibility to NIHL is genetically determined (Early et al., 2022). Research for mechanism in humans is strongly limited by genetic and environmental heterogeneity, low statistical power, and problems with long-term follow up (Early et al., 2022). Mechanistical studies in mice are therefore indispensable.

In humans, evidence is accumulating that a noise-induced PTS almost always includes cochlear synaptopathy such as loss of ribbons and/or postsynapses and thus functional auditory nerve fibers. With age, one important cause for impaired speech recognition is a gradual loss of information pathways from IHCs to the brain, especially in a noisy environment. Genetics and individual noise exposure history enhance this phenomenon (Bakay et al., 2018; Blum et al., 2024; Wu et al., 2021).

6.5   Outlook

A considerable part of the data generated for this thesis have not yet been sufficiently analysed, such as many data for the intermediate days 1, 2, 3, 5, 7, 14 and 21 as well as growth

functions and latencies of f-ABR waves II, III, IV and V. This evaluation is planned for another (theoretical) medical thesis.

Another interesting feature is the effect of biological sex on noise trauma susceptibility. CBA males were found to have higher thresholds than their female counterparts. In C57/Bl6J mice, it was the contrary (Henry, 2004). Additionally, males and females react differently to noise-induced hearing loss (Milon et al., 2018). An in-depth evaluation is currently undertaken by my medical colleague Laura Wallrich on a larger data set I contributed to.

Future experiments should always include an age-matched control group of the same size for comparison. The data of my thesis contributed a control group that was too small (4 animals) for a comparison with the 106 dB SPL- and the 112 dB SPL-treated groups. These control animals were however included in the larger control group published in (Blum et al., 2024). Finally, in future experiments on noise-induced hearing loss, DPOAE measurements should be established and included to better dissect the contribution of OHCs to threshold shifts and loss in wave I amplitudes.

7 References

Akil, O., Oursler, A.E., Fan, K., Lustig, L.R., 2016. Mouse Auditory Brainstem Response Testing. Bio-Protoc. 6. https://doi.org/10.21769/BioProtoc.1768

Anderson, L.A., Hesse, L.L., Pilati, N., Bakay, W.M.H., Alvaro, G., Large, C.H., McAlpine, D., Schaette, R., Linden, J.F., 2018. Increased spontaneous firing rates in auditory midbrain following noise exposure are specifically abolished by a Kv3 channel modulator. Hear. Res. 365, 77–89. https://doi.org/10.1016/j.heares.2018.04.012

Bakay, W.M.H., Anderson, L.A., Garcia-Lazaro, J.A., McAlpine, D., Schaette, R., 2018. Hidden hearing loss selectively impairs neural adaptation to loud sound environments. Nat. Commun. 9, 4298. https://doi.org/10.1038/s41467-018-06777-y

Blum, K., Schepsky, P., Derleder, P., Schätzle, P., Nasri, F., Fischer, P., Engel, J., Kurt, S., 2024. Noise-induced cochlear synaptopathy in C57BL/6 N mice as a function of trauma strength: ribbons are more vulnerable than postsynapses. Front. Cell. Neurosci. 18, 1465216. https://doi.org/10.3389/fncel.2024.1465216

Borg, E., Engström, B., Linde, G., Marklund, K., 1988. Eighth nerve fiber firing features in normal-hearing rabbits. Hear. Res. 36, 191–201. https://doi.org/10.1016/0378-5955(88)90061-5

Bourien, J., Tang, Y., Batrel, C., Huet, A., Lenoir, M., Ladrech, S., Desmadryl, G., Nouvian, R., Puel, J.-L., Wang, J., 2014. Contribution of auditory nerve fibers to compound action potential of the auditory nerve. J. Neurophysiol. 112, 1025–1039. https://doi.org/10.1152/jn.00738.2013

Boussaty, E.C., Gillard, D., Lavinsky, J., Salehi, P., Wang, J., Mendonça, A., Allayee, H., Manor, U., Friedman, R.A., 2020. The Genetics of Variation of the Wave 1 Amplitude of the Mouse Auditory Brainstem Response. JARO J. Assoc. Res. Otolaryngol. 21, 323–336. https://doi.org/10.1007/s10162-020-00762-3

Bramhall, N., Beach, E.F., Epp, B., Le Prell, C.G., Lopez-Poveda, E.A., Plack, C.J., Schaette, R., Verhulst, S., Canlon, B., 2019. The search for noise-induced cochlear synaptopathy in humans: Mission impossible? Hear. Res. 377, 88–103. https://doi.org/10.1016/j.heares.2019.02.016

Brask, T., 1978. The Noise Protection Effect of the Stapedius Reflex. Acta Otolaryngol. (Stockh.) 86, 116–117. https://doi.org/10.3109/00016487809123490

CDC - Noise and Hearing Loss Prevention - Reducing Noise Exposure, Guidance and Regulations - NIOSH Workplace Safety and Health Topic [WWW Document], 2018. URL https://www.cdc.gov/niosh/topics/noise/reducenoiseexposure/regsguidance.html (accessed 2.24.19).

Chen, H., Shi, L., Liu, L., Yin, S., Aiken, S., Wang, J., 2018. Noise-induced Cochlear Synaptopathy and Signal Processing Disorders. Neuroscience. https://doi.org/10.1016/j.neuroscience.2018.09.026

Chen, L., Xiong, S., Liu, Y., Shang, X., 2012. Effect of Different Gentamicin Dose on the Plasticity of the Ribbon Synapses in Cochlear Inner Hair Cells of C57BL/6J Mice. Mol. Neurobiol. 46, 487–494. https://doi.org/10.1007/s12035-012-8312-7

Cody, A.R., Johnstone, B.M., 1981. Acoustic trauma: Single neuron basis for the "half-octave shift". J. Acoust. Soc. Am. 70, 707–711. https://doi.org/10.1121/1.386906

Davis, R.R., Kozel, P., Erway, L.C., 2003. Genetic influences in individual susceptibility to noise : A review. Noise Health 5, 19.

Early, S., Du, E., Boussaty, E., Friedman, R., 2022. Genetics of noise-induced hearing loss in the mouse model. Hear. Res. 425, 108505. https://doi.org/10.1016/j.heares.2022.108505

Fettiplace, R., 2017. Hair cell transduction, tuning and synaptic transmission in the mammalian cochlea. Compr. Physiol. 7, 1197–1227. https://doi.org/10.1002/cphy.c160049

Furman, A.C., Kujawa, S.G., Liberman, M.C., 2013. Noise-induced cochlear neuropathy is selective for fibers with low spontaneous rates. J. Neurophysiol. 110, 577–586. https://doi.org/10.1152/jn.00164.2013

Geisler, C.D., 1998. From Sound to Synapse: Physiology of the Mammalian Ear. Oxford University Press, Oxford, New York.

Gnadeberg, D., Battmer, R.D., Lüllwitz, E., Laszig, R., Dybus, U., Lenarz, T., 1994. [Effect of anesthesia on the intraoperative elicited stapedius reflex]. Laryngorhinootologie. 73, 132–135. https://doi.org/10.1055/s-2007-997095

Gourévitch, B., Doisy, T., Avillac, M., Edeline, J.-M., 2009. Follow-up of latency and threshold shifts of auditory brainstem responses after single and interrupted acoustic trauma in guinea pig. Brain Res. 1304, 66–79. https://doi.org/10.1016/j.brainres.2009.09.041

Habener, S.A., Snyder, J.M., 1974. Stapedius Reflex Amplitude and Decay in Normal Hearing Ears. Arch. Otolaryngol. 100, 294–297. https://doi.org/10.1001/archotol.1974.00780040304011

Henry, K.R., 2004. Males lose hearing earlier in mouse models of late-onset age-related hearing loss; females lose hearing earlier in mouse models of early-onset hearing loss. Hear. Res. 190, 141–148. https://doi.org/10.1016/S0378-5955(03)00401-5

Jackson Laboratories, n.d. 000664 - C57BL/6J [WWW Document]. URL https://www.jax.org/strain/000664 (accessed 3.21.19).

Jongkamonwiwat, N., Ramirez, M.A., Edassery, S., Wong, A.C.Y., Yu, J., Abbott, T., Pak, K., Ryan, A.F., Savas, J.N., 2020. Noise Exposures Causing Hearing Loss Generate Proteotoxic Stress and Activate the Proteostasis Network. Cell Rep. 33, 108431. https://doi.org/10.1016/j.celrep.2020.108431

Kaur, T., Clayman, A.C., Nash, A.J., Schrader, A.D., Warchol, M.E., Ohlemiller, K.K., 2019. Lack of Fractalkine Receptor on Macrophages Impairs Spontaneous Recovery of Ribbon Synapses After Moderate Noise Trauma in C57BL/6 Mice. Front. Neurosci. 13, 620. https://doi.org/10.3389/fnins.2019.00620

Knipper, M., Zinn, C., Maier, H., Praetorius, M., Rohbock, K., Köpschall, I., Zimmermann, U., 2000. Thyroid Hormone Deficiency Before the Onset of Hearing Causes Irreversible Damage to Peripheral and Central Auditory Systems. J. Neurophysiol. 83, 3101–3112. https://doi.org/10.1152/jn.2000.83.5.3101

Kohrman, D.C., Wan, G., Cassinotti, L., Corfas, G., 2019. Hidden Hearing Loss: A Disorder with Multiple Etiologies and Mechanisms. Cold Spring Harb. Perspect. Med. a035493. https://doi.org/10.1101/cshperspect.a035493

Kujawa, S.G., Liberman, M.C., 2019. Translating animal models to human therapeutics in noise-induced and age-related hearing loss. Hear. Res. 377, 44–52. https://doi.org/10.1016/j.heares.2019.03.003

Kujawa, S.G., Liberman, M.C., 2009. Adding Insult to Injury: Cochlear Nerve Degeneration after "Temporary" Noise-Induced Hearing Loss. J. Neurosci. Off. J. Soc. Neurosci. 29, 14077–14085. https://doi.org/10.1523/JNEUROSCI.2845-09.2009

Kujawa, S.G., Liberman, M.C., 2006. Acceleration of Age-Related Hearing Loss by Early Noise Exposure: Evidence of a Misspent Youth. J. Neurosci. Off. J. Soc. Neurosci. 26, 2115–2123. https://doi.org/10.1523/JNEUROSCI.4985-05.2006

Kurt, S., 2001. Haarsinneszellschädigung durch Gentamicin im Innenohr verschiedener Mäuse-Linien (Diplomarbeit). Tübingen University.

Kurt, S., Groszer, M., Fisher, S.E., Ehret, G., 2009. Modified sound-evoked brainstem potentials in Foxp2 mutant mice. Brain Res. 1289, 30–36. https://doi.org/10.1016/j.brainres.2009.06.092

Lavinsky, J., Mendonça, A., Bressan, M., da Silva, V.A.R., Kasperbauer, G., Wang, J., Salehi, P., Boussaty, E.C., Friedman, R.A., 2021. Large-scale phenotyping of ABR P1-N1 amplitudes before and after exposure to noise in 69 strains of mice. Mamm. Genome Off. J. Int. Mamm. Genome Soc. 32, 427–434. https://doi.org/10.1007/s00335-021-09913-0

Liberman, C., 1982. Acute and chronic effects of acoustic trauma:Cochlear pathology and auditory nerve pathophysiology. New Perspect. Noise-Induc. Hear. Loss 105–134.

Liberman, M.C., 1978. Auditory-nerve response from cats raised in a low-noise chamber. J. Acoust. Soc. Am. 63, 442–455. https://doi.org/10.1121/1.381736

Liberman, M.C., Kujawa, S.G., 2017. Cochlear synaptopathy in acquired sensorineural hearing loss: Manifestations and mechanisms. Hear. Res. 349, 138–147. https://doi.org/10.1016/j.heares.2017.01.003

Liu, J., Stohl, J., Overath, T., 2024. Hidden hearing loss: Fifteen years at a glance. Hear. Res. 443, 108967. https://doi.org/10.1016/j.heares.2024.108967

Lopes, A.C., Otubo, K.A., Basso, T.C., Marinelli, É.J.I., Lauris, J.R.P., 2009. Occupational Hearing Loss: Tonal Audiometry X High Frequencies Audiometry. São Paulo 7.

Lorimer, T., Gomez, F., Stoop, R., 2015. Mammalian cochlea as a physics guided evolution-optimized hearing sensor. Sci. Rep. 5. https://doi.org/10.1038/srep12492

Mehraei, G., Hickox, A.E., Bharadwaj, H.M., Goldberg, H., Verhulst, S., Liberman, M.C., Shinn-Cunningham, B.G., 2016. Auditory Brainstem Response Latency in Noise as a Marker of Cochlear Synaptopathy. J. Neurosci. 36, 3755–3764. https://doi.org/10.1523/JNEUROSCI.4460-15.2016

Mianné, J., Chessum, L., Kumar, S., Aguilar, C., Codner, G., Hutchison, M., Parker, A., Mallon, A.-M., Wells, S., Simon, M.M., Teboul, L., Brown, S.D.M., Bowl, M.R., 2016. Correction of the auditory phenotype in C57BL/6N mice via CRISPR/Cas9-mediated homology directed repair. Genome Med. 8, 16. https://doi.org/10.1186/s13073-016-0273-4

Milon, B., Mitra, S., Song, Y., Margulies, Z., Casserly, R., Drake, V., Mong, J.A., Depireux, D.A., Hertzano, R., 2018. The impact of biological sex on the response to noise and otoprotective therapies against acoustic injury in mice. Biol. Sex Differ. 9. https://doi.org/10.1186/s13293-018-0171-0

Milon, B., Shulman, E.D., So, K.S., Cederroth, C.R., Lipford, E.L., Sperber, M., Sellon, J.B., Sarlus, H., Pregernig, G., Shuster, B., Song, Y., Mitra, S., Orvis, J., Margulies, Z., Ogawa, Y., Shults, C., Depireux, D.A., Palermo, A.T., Canlon, B., Burns, J., Elkon, R., Hertzano, R., 2021. A cell-type-specific atlas of the inner ear transcriptional response to acoustic trauma. Cell Rep. 36, 109758. https://doi.org/10.1016/j.celrep.2021.109758

Müller, M., Hünerbein, K. von, Hoidis, S., Smolders, J.W.T., 2005. A physiological place–frequency map of the cochlea in the CBA/J mouse. Hear. Res. 202, 63–73. https://doi.org/10.1016/j.heares.2004.08.011

Murillo-Cuesta, S., Camarero, G., González-Rodríguez, A., De La Rosa, L.R., Burks, D.J., Avendaño, C., Valverde, A.M., Varela-Nieto, I., 2012. Insulin receptor substrate 2 (IRS2)-deficient mice show sensorineural hearing loss that is delayed by concomitant protein tyrosine phosphatase 1B (PTP1B) loss of function. Mol. Med. Camb. Mass 18, 260–269. https://doi.org/10.2119/molmed.2011.00328

Nasri, F., 2023. Auswirkungen eines Schalltraumas auf das Hörvermögen von Mäusen mit modifiziertem Cav1.3-Calciumkanal (Cav1.3DCRDHA/HA) in Haarsinneszellen. (Dissertation Humanmedizin). Universität des Saarlandes, Homburg.

Natarajan, N., Batts, S., Stankovic, K.M., 2023. Noise-Induced Hearing Loss. J. Clin. Med. 12, 2347. https://doi.org/10.3390/jcm12062347

NIOSH, 2012. NIOSHTIC [WWW Document]. URL https://www.cdc.gov/niosh/nioshtic-2/20041671.html (accessed 3.3.19).

Ohlemiller, K.K., 2019. Mouse methods and models for studies in hearing. J. Acoust. Soc. Am. 146, 3668–3680. https://doi.org/10.1121/1.5132550

Petitpré, C., Wu, H., Sharma, A., Tokarska, A., Fontanet, P., Wang, Y., Helmbacher, F., Yackle, K., Silberberg, G., Hadjab, S., Lallemend, F., 2018. Neuronal heterogeneity and stereotyped connectivity in the auditory afferent system. Nat. Commun. 9, 3691. https://doi.org/10.1038/s41467-018-06033-3

Pickles, J., 2013. An Introduction to the Physiology of Hearing: Fourth Edition. BRILL.

Pujol, R., Puel, J.-L., D'aldin, C.G., Eybalin, M., 1993. Pathophysiology of the Glutamatergic Synapses in the Cochlea. Acta Otolaryngol. (Stockh.) 113, 330–334. https://doi.org/10.3109/00016489309135819

Reijntjes, D.O.J., Köppl, C., Pyott, S.J., 2020. Volume gradients in inner hair cell-auditory nerve fiber pre- and postsynaptic proteins differ across mouse strains. Hear. Res. 390, 107933. https://doi.org/10.1016/j.heares.2020.107933

Reynolds, R.P., Kinard, W.L., Degraff, J.J., Leverage, N., Norton, J.N., 2010. Noise in a Laboratory Animal Facility from the Human and Mouse Perspectives. J. Am. Assoc. Lab. Anim. Sci. JAALAS 49, 592–597.

Rosenhall, U.L., Lidén, G., Nilsson, E.V., 1979. STAPEDIUS REFLEX DECAY IN NORMAL HEARING SUBJECTS. Ear Hear. 4, 157.

Rüttiger, L., Zimmermann, U., Knipper, M., 2017. Biomarkers for Hearing Dysfunction: Facts and Outlook. ORL 79, 93–111. https://doi.org/10.1159/000455705

Schaette, R., McAlpine, D., 2011. Tinnitus with a Normal Audiogram: Physiological Evidence for Hidden Hearing Loss and Computational Model. J. Neurosci. 31, 13452–13457. https://doi.org/10.1523/JNEUROSCI.2156-11.2011

Schätzle, P., unpublished. Doctoral thesis.

Schmiedt, R.A., 1989. Spontaneous rates, thresholds and tuning of auditory-nerve fibers in the gerbil: Comparisons to cat data. Hear. Res. 42, 23–35. https://doi.org/10.1016/0378-5955(89)90115-9

Scimemi, P., Santarelli, R., Selmo, A., Mammano, F., 2014. Auditory brainstem responses to clicks and tone bursts in C57 BL/6J mice. Acta Otorhinolaryngol. Ital. 34, 264–271.

Sergeyenko, Y., Lall, K., Liberman, M.C., Kujawa, S.G., 2013. Age-related cochlear synaptopathy: an early-onset contributor to auditory functional decline. J. Neurosci. Off. J. Soc. Neurosci. 33, 13686–13694. https://doi.org/10.1523/JNEUROSCI.1783-13.2013

Shi, L., Liu, K., Wang, H., Zhang, Y., Hong, Z., Wang, M., Wang, X., Jiang, X., Yang, S., 2015. Noise induced reversible changes of cochlear ribbon synapses contribute to temporary hearing loss in mice. Acta Otolaryngol. (Stockh.) 135, 1093–1102. https://doi.org/10.3109/00016489.2015.1061699

Shrestha, B.R., Chia, C., Wu, L., Kujawa, S.G., Liberman, M.C., Goodrich, L.V., 2018. Sensory neuron diversity in the inner ear is shaped by activity. Cell 174, 1229-1246.e17. https://doi.org/10.1016/j.cell.2018.07.007

Snow, J.B., Wackym, P.A., Ballenger, J.J., 2009. Ballenger's Otorhinolaryngology: Head and Neck Surgery, Otorhinolaryngology: Head and Neck Surgery. BC Decker.

Song, Q., Shen, P., Li, X., Shi, L., Liu, L., Wang, Jiping, Yu, Z., Stephen, K., Aiken, S., Yin, S., Wang, Jian, 2016. Coding deficits in hidden hearing loss induced by noise: the nature and impacts. Sci. Rep. 6. https://doi.org/10.1038/srep25200

Sun, S., Babola, T., Pregernig, G., So, K., Nguyen, M., Su, M., Palermo, A., Bergles, D.E., Burns, J.C., Müller, U., 2018. Hair Cell Mechanotransduction Regulates Spontaneous Activity and Spiral Ganglion Subtype Specification in the Auditory System. Cell 174, 1247-1263.e15. https://doi.org/10.1016/j.cell.2018.07.008

Suthakar, K., Liberman, M.C., 2021. Auditory-nerve responses in mice with noise-induced cochlear synaptopathy. J. Neurophysiol. 126, 2027–2038. https://doi.org/10.1152/jn.00342.2021

Takazawa, T., Ikeda, K., Murata, K., Kawase, Y., Hirayama, T., Ohtsu, M., Harada, H., Totani, T., Sugiyama, K., Kawabe, K., Kano, O., Iwasaki, Y., 2012. Sudden Deafness and Facial Diplegia in Guillain-Barr^|^eacute; Syndrome: Radiological Depiction of Facial and Acoustic Nerve Lesions. Intern. Med. 51, 2433–2437. https://doi.org/10.2169/internalmedicine.51.7737

Trautwein, P., Hofstetter, P., Wang, J., Salvi, R., Nostrant, A., 1996. Selective inner hair cell loss does not alter distortion product otoacoustic emissions. Hear. Res. 96, 71–82. https://doi.org/10.1016/0378-5955(96)00040-8

Tsuji, J., Liberman, M.C., 1997. Intracellular labeling of auditory nerve fibers in guinea pig: central and peripheral projections. J. Comp. Neurol. 381, 188–202. https://doi.org/10.1002/(SICI)1096-9861(19970505)381:2<188::AID-CNE6>3.0.CO;2-#

Vettorazzi, S., Nalbantoglu, D., Gebhardt, J.C.M., Tuckermann, J., 2022. A guide to changing paradigms of glucocorticoid receptor function-a model system for genome regulation and physiology. FEBS J. 289, 5718–5743. https://doi.org/10.1111/febs.16100

Wang, Y., Hirose, K., Liberman, M.C., 2002. Dynamics of Noise-Induced Cellular Injury and Repair in the Mouse Cochlea. JARO J. Assoc. Res. Otolaryngol. 3, 248–268. https://doi.org/10.1007/s101620020028

Wang, Y., Liberman, M.C., 2002. Restraint stress and protection from acoustic injury in mice. Hear. Res. 165, 96–102. https://doi.org/10.1016/S0378-5955(02)00289-7

Wu, P.-Z., O'Malley, J.T., de Gruttola, V., Liberman, M.C., 2021. Primary Neural Degeneration in Noise-Exposed Human Cochleas: Correlations with Outer Hair Cell Loss and Word-Discrimination Scores. J. Neurosci. Off. J. Soc. Neurosci. 41, 4439–4447. https://doi.org/10.1523/JNEUROSCI.3238-20.2021

Yoshida, N., Hequembourg, S.J., Atencio, C.A., Rosowski, J.J., Liberman, M.C., 2000. Acoustic injury in mice: 129/SvEv is exceptionally resistant to noise-induced hearing loss. Hear. Res. 141, 97–106. https://doi.org/10.1016/S0378-5955(99)00210-5

Zhou, X., Jen, P.H.-S., Seburn, K.L., Frankel, W.N., Zheng, Q.Y., 2006. Auditory brainstem responses in 10 inbred strains of mice. Brain Res. 1091, 16–26. https://doi.org/10.1016/j.brainres.2006.01.107

8 Annex: Supplementary information
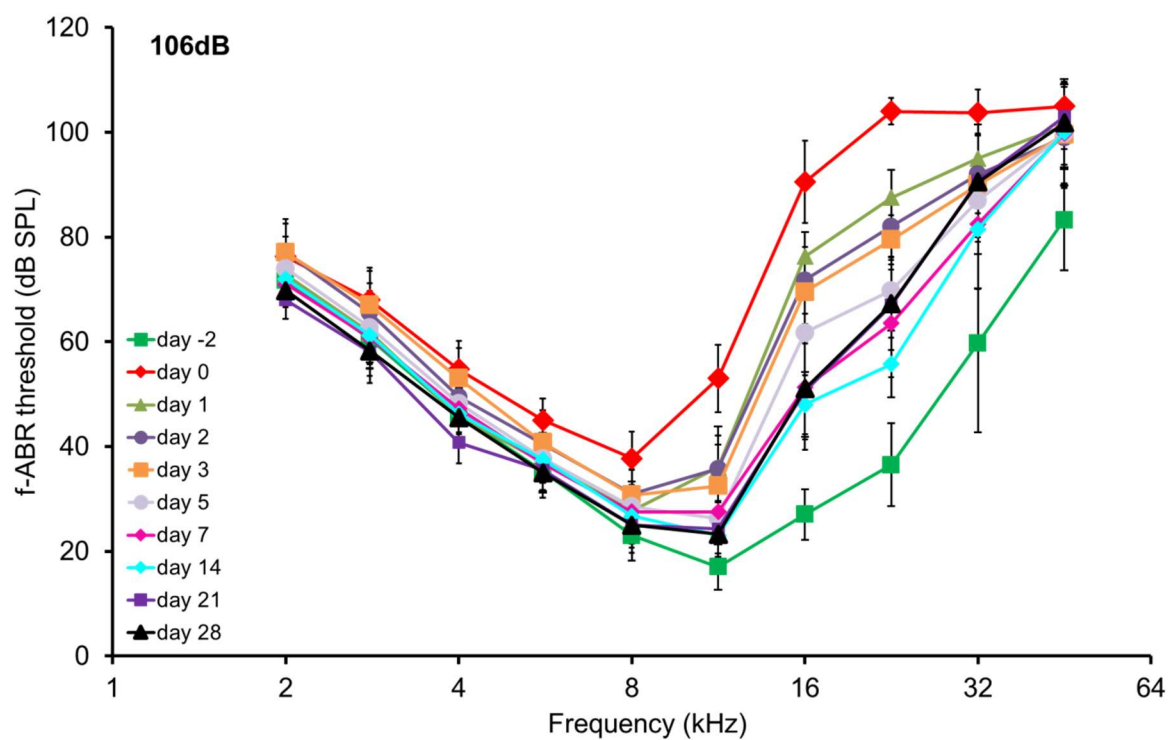
Figure 32. Effects of the 106 dB SPL trauma on mean f-ABR thresholds for all days of ABR recordings. N = 20 ears.
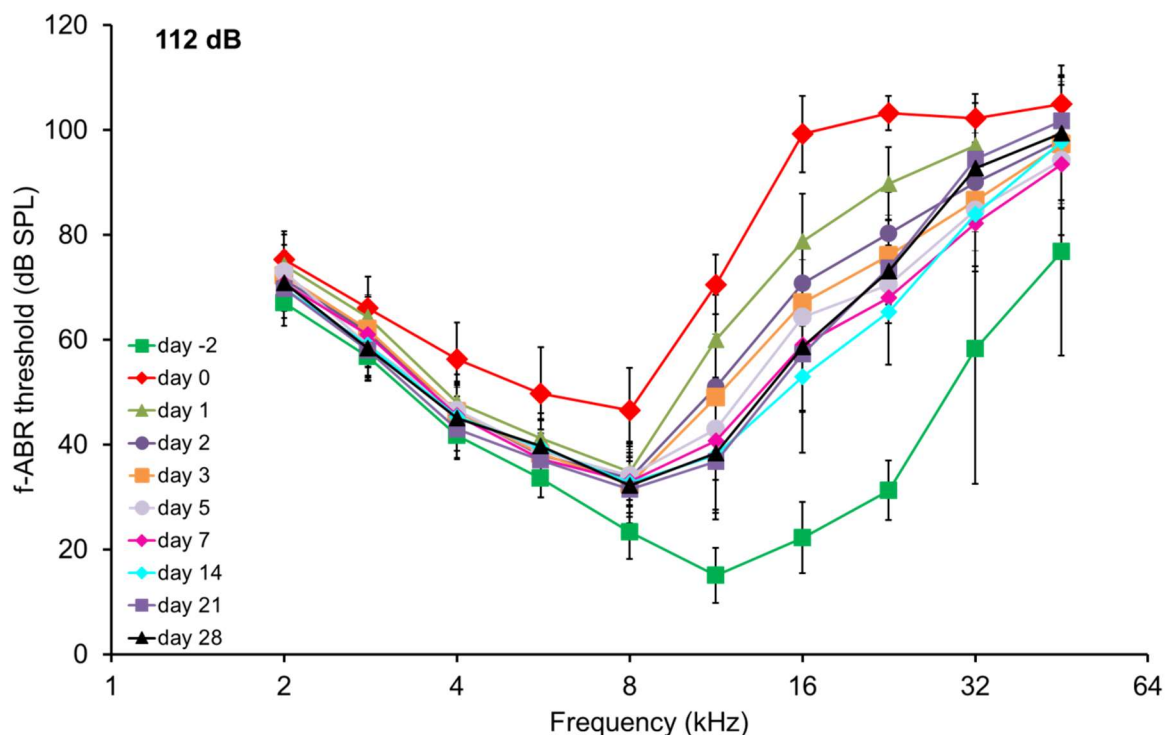
Figure 33. Effects of the 112 dB SPL trauma on mean f-ABR thresholds for all days of ABR recordings. N = 20 ears, except for day 28 (n = 18 ears).

Table 16. Detailed pair analysis of the Friedman/Bonferroni test between day -2 versus any post-traumatic day of latencies in waves I-V in the two trauma groups. Out of 50 pairs, only four showed significant differences. All are found in the 106 dB SPL trauma group. Three increases of latency (in red) are found in wave I, one decrease of latency (in green) is found in wave II.

106 dB SPL wave I

p-value	day-2	day0	day1	day3	day14	day28
day-2	ns	<0.001	ns	<0.001	<0.001	ns

106 dB SPL wave II

p-value	day-2	day0	day1	day3	day14	day28
day-2	ns	ns	0.009	ns	ns	ns

9 C.V.

Aus datenschutzrechtlichen Gründen wird der Lebenslauf in der elektronischen Fassung der Dissertation nicht veröffentlicht.

10 Acknowledgments

Tag der Promotion: 24.07.2025

Dekan: Prof. Dr. med. dent. Matthias Hannig

Berichterstatter: Prof. Dr. Jutta Engel

      Prof. Dr. Maximilian Linxweiler